Impact of Second-Life Batteries on Enhancing the Integration of Renewable Energy Resources

by

Engy Adel Mohamed Mohamed Hassan

A thesis
presented to the University of Waterloo
in fulfillment of the
thesis requirement for the degree of
Master of Applied Science
in
Electrical and Computer Engineering

Waterloo, Ontario, Canada, 2019

AUTHOR'S DECLARATION

I hereby declare that I am the sole author of this thesis. This is a true copy of the thesis, including any required final revisions, as accepted by my examiners.

I understand that my thesis may be made electronically available to the public.

Abstract

The current distribution systems are typically not designed to accommodate a high level of renewable sources. Customer impact assessment studies are usually required by the distribution utility prior to the connection of DG. In these studies, the impacts of Distributed Generator (DG) on the system voltage profile, reverse power flow, short circuit level, and the system voltage unbalance are evaluated. If the DG failed to fulfill the distribution system technical requirement, the DG project application might be rejected. In some cases, the DG capacity may be reduced to fulfill the technical constraints. In other cases, the renewable based DG power may be curtailed (especially at peak generation). The reduction in DG capacity, as well as the DG active power curtailment, will badly affect the DG project investment.

In order to eliminate the DG active power curtailment, the investor may connect a battery at the same point of the renewable DG. The battery can dispatch the DG generation; therefore, the peak DG power, that causes the violation to the system technical constraints, is shaved. However, the high capital cost of the batteries may negatively affect the investor profit. In such cases, the usage of second life (SL) batteries represents the most useful solution. SL batteries have significantly cheaper capital costs compared to new batteries. Thereby, the major driver for using SL batteries is the possibility of reducing costs and maximizing the DG investment by avoiding the utilization of new Li-ion batteries.

The main aim of this research is to use batteries, which have lost part of their original performance during their first life, with the distribution system applications. The general objective is to utilize the SL batteries for smoothing the photovoltaic based DG power to increase the DG penetration while fulfilling the utility technical constraints. Another objective is to use the SL batteries connected at the same bus of the DG to maximize the DG project investment.

Towards the execution of the proposed research work, some ancillary studies are presented in chapter (3); the results of these studies are used to solve the main problems under study presented in chapter (4). The studies presented in Chapter (3) comprises a probabilistic model for the PV DG, a long-term forecasting technique for the system load, a load flow study to determine the maximum allowable injected DG power, and an economic assessment study to determine the best PV DG capacity that increases the net present value of the profit of the PV DG project.

The results of the aforementioned studies are integrated with the main problems under study that were formulated and solved in Chapter (4). Two main objectives were presented in this chapter; i.e. the first objective is to obtain the optimal size of the SL batteries that achieve zero curtailment while minimizing the battery cost, the second objective is to obtain the optimal schedule of the batteries that maximize the net present value of the profit.

The results obtained show that the SL batteries are adequate for the application, and they have superiority over the brand-new batteries in terms of cost. SLB batteries give a chance to the investor to purchase batteries at low prices at later years of the project rather than purchasing all the required batteries at the beginning of the project. Thus, the SL batteries offer a competitive solution for the cost problems associated with the battery integration with the distribution systems.

Acknowledgments

First and foremost, all praises to Allah Almighty for providing me with the opportunity, patience, and guidance to finalize this thesis work and my MASc degree successfully.

I would like to express my deep appreciation and gratitude to my advisors Prof. Magdy Salama and Prof. Mohamed Ahmed for their invaluable guidance, limitless support, and continual encouragement. Throughout my MASc journey, their advice was the key to direct this research on the right path.

Dedication

To my father and his precious soul, to my mother, to my beloved husband Mahmoud in recognition of his endless support, dedication, and encouragement, and finally for my two little sons Abelrahman and Nourelden.

Table of Contents

List of Figures

List of Tables

Chapter (1)
Introduction

1.1 General

In the last few decades, the renewable based Distributed Generators (DGs) have been extensively integrated with the distribution network due to the increased environmental and economic benefits. DGs play an important role in reinforcing the main substations to satisfy the swelling demand. DGs can be connected or disconnected easily from the network, thus providing higher flexibility. Properly planned and operated DG installations have many benefits as savings due to decreasing system power loss, system reliability and security enhancement, Power Quality improvements, emissions reduction due to the usage of Renewable Energy Sources (RES).

Despite the multiple economic and environmental benefits that integration of RES offers to the distribution network, the integration of RES also raises several uncertainty issues for the distribution system due to the intermittent nature of these RES. The RES are strongly correlated to the climate, ambient temperature, season, time, and geography; thus, they follow a stochastic distribution pattern dependent on their primary sources and the generation technologies.

Several solutions were offered to mitigate the impacts of RES high variability; the most prominent solution to connect battery energy storage systems (BESS) at the same point of the RES. BESS can provide smoothing for the RES power so that the RES power can be dispatched on an hourly basis based on the forecasted conditions. In addition, the BESS could be used to maximize the total net profit of the DG investment project by allowing higher DG power without violating the distribution system technical constraints.

On the other hand, the Electric vehicles (EVs) witness an evolution in the latest few decades.. Due to this evolution it is expected that in the upcoming few decades a massive amount of second life electric vehicles batteries are required to be retired from the automotive life. However, the automotive end of life doesn't mean that the battery can't be used in further applications. In the automotive application the EV battery is considered to be inefficient when the capacity reaches 70-80 % of its original capacity. However, the degraded capacity of the second life battery is still making it beneficial in some electric grid application.

Applications of the SL battery in the electric grid should be analyzed economically; this is because the planner has the choice either to install one brand new battery that will not suffer a high degradation along the project lifetime or to use multiple SL batteries installed at different years of the project lifetime. This thesis is handling the idea of using the second life batteries for increasing the penetration of PV DG, minimizing the DG active power curtailment, and maximizing the total income of the DG investement. Chapter 1 of this dissertation presents the main motivations of this work, the overall objectives of the presented research, and the outline of this thesis.

1.2 Motivation

The connection of RES to the distribution network is technically constrained as the current distribution systems are typically not designed to accommodate a high level of renewable DG sources. Customer impact assessment (CIA) studies are usually required by the distribution utility prior to the connection of DG. In these studies, the impacts of DG on the system voltage profile, reverse power flow, short circuit level, and the system voltage unbalance are evaluated. If the DG failed to fulfill the distribution system technical requirement, the DG project application might be rejected. In some cases, the DG capacity may be reduced in order to achieve the technical constraints. In other cases, the renewable based DG power may be curtailed (especially at peak generation). The reduction in DG capacity, as well as the DG active power curtailment, will badly affect the DG project investment.

To eliminate the DG active power curtailment, the investor may connect BESS at the same point of the renewable DG. The BESS can dispatch the DG generation; therefore, the peak DG power, that causes the violation to the system technical constraints, is shaved. In addition, in case of the net metering type of connection, the BESS could be used for increasing the DG investment profit by storing energy at off-peak periods and releasing that energy at the peak periods.

Despite all the aforementioned benefits, the net effect of BESS on the DG project investment may be negative due to the high BESS capital cost. Moreover, the system restriction on the DG penetration level could be alleviated over the project lifetime. For example, due to the growth of the distribution feeder loads, the utility may decide to expand its substations capacity or even build a new substation. Another alternative is to encourage customers to participate in Customer Demand Management (CDM) and Distributed Energy Resources (DER) programs. In other words, the utility may allow more DG penetration to meet the growing demand. Therefore, in this case, the BESS will be used only for the first few years of the project lifetime.

In such cases, the usage of second life (SL) batteries represents the most useful solution. Second life batteries have significantly cheaper capital costs compared to new batteries, and their reduced lifetime, the main disadvantage of these batteries is an advantage in this case. Thereby, the major driver for using SL batteries (retired from their first life automotive service) is the possibility of reducing costs and maximizing the DG investment by avoiding the utilization of new Li-ion batteries.

Another motivation for this research is its environmental impact. The usage of SL batteries in smoothing the RES power will achieve several environmental benefits at the same time; the increased renewable power penetration will decrease the usage of fossil fuels. Moreover, the usage of SL batteries will minimize the environmental impacts; by avoiding the manufacturing of new batteries to cover the same application. Furthermore, due to the proliferated penetration of Electric Vehicles nowadays, thousands of SL batteries will be present during the next decade. these batteries should be employed in beneficial application and avoid the negative environmental impact of the batteries disposal.

1.3 Research Objectives

This research work aims to use batteries, which have lost part of their original performance during their first life, with the distribution system applications. The general objective is to utilize the SL batteries for smoothing the photovoltaic based DG power in order to increase the DG penetration while fulfilling the utility technical constraints. Another objective is to use the SL batteries connected at the same bus of the DG to maximize the DG project investment.

The specific objectives of the presented work are discussed as follows;

- Develop a long-term load forecasting technique in order to forecast the distribution system loading conditions
- Develop a probabilistic modeling strategy for photovoltaic based DGs that considers their stochastic nature.
- Determine the DG capacity that maximizes the net present value (NPV) of the DG investment profit while maintaining the distribution system technical constraints.

- Obtain the optimal capacity and the operation schedule of the SL batteries required to minimize the DG active power curtailment and to maximize the DG investment profit

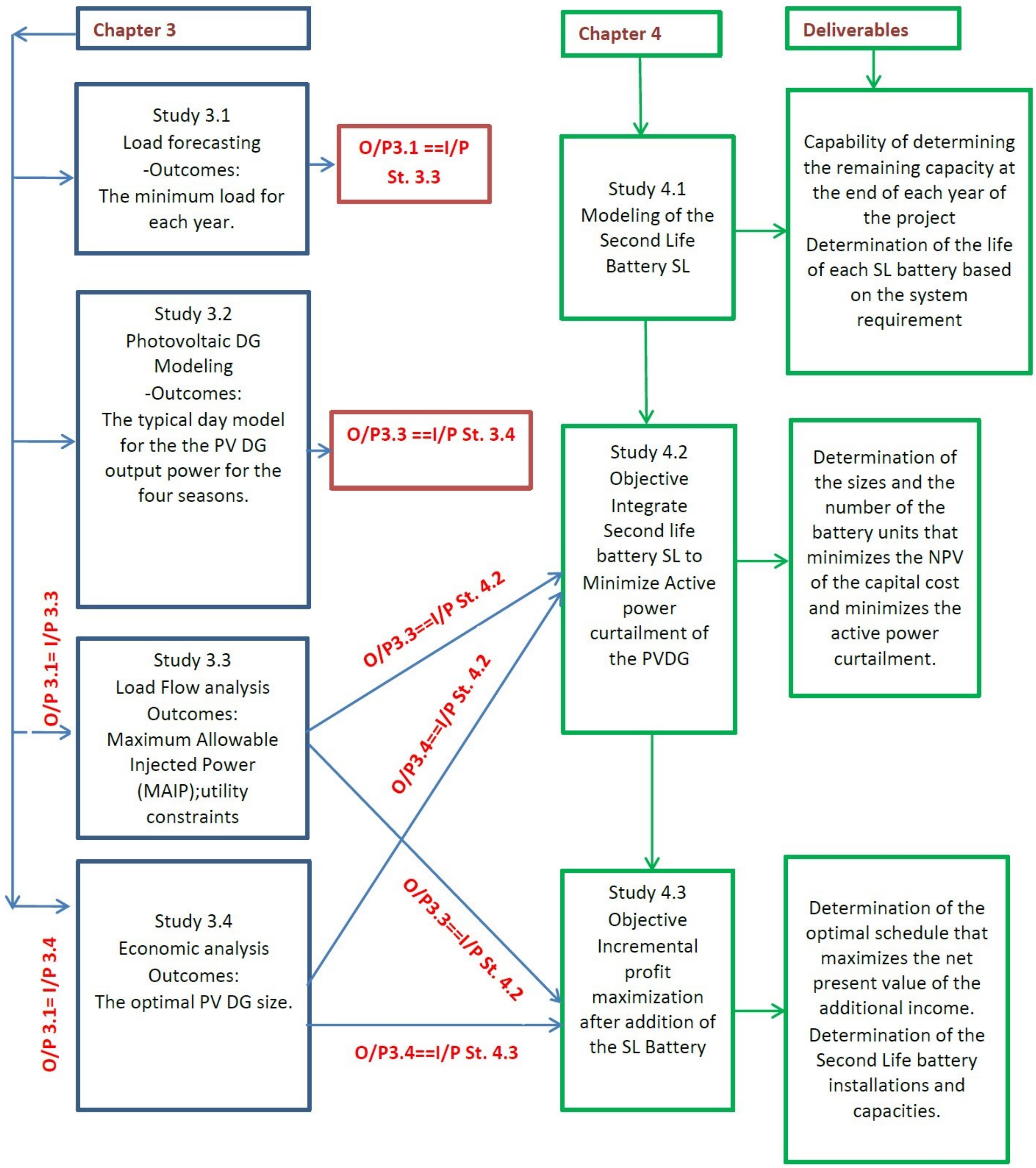

Figure 1.1 Thesis organization chart

1.4 Thesis Organization

The proposed research in this thesis deals with the utilization of SL batteries for maximizing the photovoltaic DG investment profit while satisfying the system technical constraints. This thesis organization is shown in fig 1.1 and illustrated as follows;

- In chapter (1), a brief introduction to the BESS integration with the distribution system is presented. Moreover, the thesis motivations, objectives, and organization are listed.
- In chapter (2), a quick survey on the Energy Storage Systems (ESS) is presented. The survey focuses on the Battery Energy Storage Systems BESS. In addition, the chapter presented a detailed review of the SL batteries performance parameters and expected lifetime as well as their potential applications.
- In chapter (3), the probabilistic model of the photovoltaic based DGs is presented, and the long-term load forecasting technique is proposed. Moreover, the DG capacity selection technique for achieving the maximum investment profit is presented.
- In chapter (4), the SL batteries Usage with the distribution system is studied; the optimization problem is formulated and solved. Furthermore, the results are presented and discussed.
- In chapter (5), a summary of the presented research, and contributions are presented. The recommendations for further work are provided.

Chapter 2
Literature Review

2.1 Introduction

The renewable energy sources (RES) penetration in the power system is increasing because of its role in minimizing the negative environmental impacts of conventional fossil fuel-based technologies. However, the stochastic nature of the renewables creates high uncertainty in the energy production profile which makes it difficult for power system operators to rely on the RES in the power system and market operation. Thus, the energy storage systems (ESSs) are utilized to decrease the uncertainties associated with the RES. ESSs are important for voltage and power smoothing, as well as load leveling, peak shaving, energy management, and frequency regulation, also may be used as a standby generation during faults.

On the level of the distribution systems based on the capacities, the utilized energy storage systems are battery-based energy storage systems (BESS). BESS has numerous applications in the distribution systems. However, the most common application from the customers or investors point of view is to maximize the benefits by using the BESS as arbitrage; in which the energy is stored in the off-peak times; when the energy cost is minimal and injected during the peak hours; when the energy cost is high. In the previous scenario, the utility seems to be losing the energy cost at the system peak. However, the utility function is to guarantee high quality and the continuity of the power supplied to the customers. It would be preferable for the utility to take off the shoulders the running and fixed the cost of establishing new power plants or even operating the existing plants with light loading to solve the congestions problems. In this case, the injected power coming from compatible renewable-ESS will manage to offer energy with good quality and reasonable prices to the system.

Several studies were carried out on the ESS to minimize its cost; either by developing less expensive materials or by creating ESS with higher energy density. However, ESS is still having high relative costs; which discourage the customers and the distribution system investors to integrate them with RES based generators; especially on the small scale investments. The aforementioned reason makes the second life batteries usage in the power system is a promising application; especially for the applications with light consumption compared to the automotive application; such as the electric grid. However; not all the second life batteries could be installed in the power system. According to the previous studies; the most important specs that should be considered while choosing a second life battery is the percentage fading of the capacity, the rate of charge and discharge during the first-hand usage, the remaining lifetime, the state of health, the percentage deterioration of the efficiency, and depth of discharge (DOD). All of these parameters should be considered during the modeling and adopting of the second life battery in the power system applications.

This remaining of this chapter is organized as follows; section 2 introduces a general overview of different technologies of energy storage systems, and the applicability of each technology to the distribution system Section 3 focuses on the second life batteries and the main parameters and specifications that should be considered while choosing a second life electric vehicle battery in the distribution systems.

2.2 Energy storage system technologies

Energy storage technologies are based on storing the electrical energy in some forms and then retransform it into electric energy whenever needed. ESS can be categorized based on different aspects; such as the duration (short or long term), the type of the converted energy, or other criteria such as the efficiency, capacity and the capital cost or the impact on the environment. the surveyed EES technologies includes Pumped Hydro Systems (PHS) [1]-[5], Compressed Air Energy Storage (CAES) [5]-[9], flying wheel energy storage [10]-[13], and Battery Energy Storage Systems (BESS), Supercapacitors/ Ultracapacitors [2], [3], [8], Superconducting Magnetic Energy Storage (SMES) [13], [2], [20], [21] ,and Hydrogen Energy Storage HES - Fuel Cells FC [2], [6], [13], [8], [5], [15]. The following section highlights the battery energy storage systems.

2.2.1 Battery Energy Storage Systems

Batteries are considered as the most well-known energy storage devices. In addition, they are configured as long-term energy storage devices. Batteries have high combinational flexibility to fit different loadings capacities as the battery cells could be connected in series and/or in parallel to match any loading profile.

Table 2-1 The main characteristics advantages and disadvantages of chemical batteries

	Lead acid	Ni-based	Sodium-sulfur	Sodium Nickel Chloride	Lithium-ion	Flow batteries
Lifetime	2-3 years	10-15	10–15	10-14	20 years	20 years
Cost $/kwh	150–500	800–1500	300–500	150-300	600–2500	NI
Efficiency	65–80%	60-70%	75–90%	90%	90–97%	60-85%
Time response	Fast <5msec	<5ms	Fast <5msec	<5ms	Fast <5msec	NI
Advantage	➢ High reliability and sustainability for power quality& spinning reserve. ➢ Low self-discharge rate<0.3% /day	➢ Low maintenance cost. ➢ Good performance at low temperatures	➢ High rated capacity 244.8MWh. ➢ Low maintenance need. ➢ Nontoxic material. ➢ 99% recyclable.	➢ No maintenance cost. ➢ Very low self-discharge	➢ low maintenance required. ➢ Power density is relatively high ➢ Better performance at low temp. ➢ Low self-discharge rate <5%/yr	➢ No self-discharge rate. ➢ No effect after deep discharge. ➢ Long lifetime. ➢ Low maintenance rate. ➢ Can reach to 100% DoD
Disadv.	➢ Low energy density. ➢ Low specific power. ➢ Limited life cycles. ➢ High maintenance requirement. ➢ Emits explosive gases. ➢ Slow charge	➢ Harmful to environment ➢ Maximum capacity decreases dramatically ➢ High cost	➢ High operating cost ($80/kW/year) ➢ Explosion hazards are possible. ➢ The initial capital cost is high	➢ low potential in power system application	➢ The lifetime of the Li-ion is based on the operating temperature. ➢ Toxicity due to metal oxide electrodes if overcharging or over discharging	➢ High investment cost.

Batteries could be categorized into two main types; electrochemical and redox flow batteries (reduction-oxidation). Both of them are based on the chemical reactions; however, the techniques used in the chemical reactions are different. The main concept is the transformation of the direct current to chemical energy stored. Where the criteria the batteries store energy is by creating an ionic potential difference between the positive and negative plates with dielectric material in between to facilitate the mobility of the charges. In other words, during the charging process, the electric energy is transformed into chemical energy and during the discharge, the process is reversed taking into consideration that the flow of the electrons is fixed DC current. Table 2-1 summarizes the types of BESS, their characteristics, efficiency, time response, and pros. and cons.

2.3 Second Life (SL) Batteries

The idea of SL batteries was aroused from the predicted growth of the electric vehicles in the upcoming years. Moreover, it was one of the solutions to maximize the salvage cost of the electric batteries which is considered to have a relatively high cost. The studies carried on this topic analyze the problems from different perspectives. Some studies are carried to determine the appropriate retirement time from automotive life to maximize the benefits. Other studies handled the reliability assessment of the SL batteries. In addition, some studies were carried out to handle the profitability of SL batteries. The following subsections discuss the idea of integrating the SL batteries in the active distribution networks, the parameters estimation, and the economic worth of adopting the second life batteries. In addition, different modeling techniques are presented to estimate the capacity of the SL batteries along the project's life span

2.3.1 Parameters Affecting the Capacity Fading in SL Batteries

The following parameters affect the capacity fading in SL batteries:

- State of health (SOH): it is the figure of merit of the battery compared to the mint condition. That includes any changes in the capacity or the internal parameters (e.g. capacitance, resistance)
- State of charge (SOC): is the percentage charge of the battery.
- Depth of discharge (DOD): is complimentary of the SOC, and it is advised by the manufacturer that it should be kept between 80% and 20%.
- C-Rate: the ampere-hour charge and discharge per unit time

- Deterioration rate: the percentage of the capacity fade based on the time storage or the variation in the temperature.
- Temperature: the ideal operation condition of the battery ranges between -20C and 60C, the performance is affected by the higher and lower temperatures.

Number of complete discharges: this parameter causes damage to the battery and affects its life. Most of the modeling considering the capacity fading considers a number of complete discharges.

2.3.2 Grid Applications of the SL Batteries

Electric vehicles (EV) among its types plugged in hybrid electric vehicles invaded the market in the last decade, and it is expected to keep growing through the upcoming decades. The viability of the EV is contingent on the predicted economic value of the electric vehicle batteries. In spite of the positive environmental impact of the electric vehicles; the costs are relatively high. This was an impetus for the government to encourage the academic and practical projects to propose solutions that aim to increase the density of the batteries, as well as, the reduction of its cost. The EV manufacturers recommended the replacement of the EV batteries after capacity fade from 20-30%. This condition acted as an inspiration to the researchers in the electric field; as the characteristics of the EV after retirement matches some of the applications in the electric grid [36], [37]. The deterioration rate of the EV batteries returns to the exposure of the EVs to different climatic variations and consequently temperatures, Moreover, there is no a fixed pattern for the rate of discharging or the depth of discharging even with the advised directions of the manufacturers. This is not the case in the applications of the electric grid and the ancillary services; where the temperature is almost fixed and the pattern varies by the variation of the application but it still almost fixed. In addition to the remarkable difference between the new and the SL electric batteries; SL batteries are interesting material for research. The following applications area carried practically through different projects.

1. The assistance of the ancillary systems

The prominent application of the SL batteries are assisting the ancillary services; such as system balancing, spinning reserve and load following. Moreover, it could be applied in the smoothing of the energy penetration of renewable energy resources; either on the transmission level or on the distribution small scale level.

2. Assisting EV fast chargers

In [36], an actual project was executed in which the SL batteries are used in fast EV charge; in which three fast EV chargers were connected and a grid connection of 70 kW power peak. Because of the lack in the power at the schedule, the project added SL batteries for assistance.

3. Self-consumption

In this case, the promising applications of smart energy management inside buildings are aroused. The SL batteries have a bright future in the projects of the net-zero metering or even the small-scale assistance of existing rooftop PV generators. On land small scale project was carried that assisted the generation of PV Based generator with 6 kWh through SL batteries [36].

4. Area regulation:

The area regulation is an additional service that the owner of the self- consumption can add when there is a surplus in the energy. Hence, area regulation is added to the self-consumption current profile which ends up with higher energy exchange.

5. Transmission Deferral

In this application, the power is transmitted from one grid to neighbor grid transformer; it happens when the energy demand is higher than the transformer capability. Where the batteries charge during the off-peak periods and re-supply the power on demand. The main advantage of this application is the deferral of the transformer upgrade time.

2.3.3 Economic Benefits of the SL Batteries

Many studies were carried out to handle the economic benefits of SL batteries. The outcomes of these studies provided different conclusions; some are supporting the integration of the SL batteries with the system, while others are against this integration. It can be concluded that the SL batteries economic benefits should be evaluated based on numerous factors such as the application and the battery need for refurbishment. The following subsections discuss different point of views based on the economic benefits and the profitability of the SL batteries.

2.3.3.1 Calculating the Market Price of the SL Battery [38]-[42]

In order to calculate the market price SL battery, some parameters should be considered such as the state of health, the capacity fade, the number of cycles in the first life, the remaining life span after the first life. The evaluation in most of the studies is based on tracking the performance of the first life, determining the total life cycles (rate of discharges) and the depth of the discharge determined by the manufacturer in the whole life of the of the EV battery, and monitor the average number of cycles at which the capacity remaining is between 70-80%. In order to evaluate an approximate range of the cost of the SL battery, based on the aforementioned items, a ratio between the first life cycles consumption and the total determined manufacturer cycles is calculated and multiplied by the cost of the new battery. The ratio takes into consideration the deterioration occurred due to the number of cycles in the first life and the state of health after being retired from the automotive life. Some of the studies subtracted an incentive value to encourage the investment of the SL batteries if compared to the new ones. In addition, in other studies, the refurbishment cost is added.

2.3.3.2 The Profitability of Integrating the SL Battery

The profitability of the SL battery is the benefits that the investor acquires from using such technologies. Thus, the study should consider two main points. First, the applications in which the customer has invested. Second, the study should include a comparison between the usages of the brand-new batteries and the SL battery. In [43], eighteen applications were illustrated to the profit applications in the SL battery. Moreover, the combination of these applications was mixed to maximize the profit.

2.3.3.3 Market Potential to Adopt the SL Batteries

The investors would be oriented towards the most profitable applications of the SL batteries. With the expected linear growth of the EV, the SL batteries will grow as well. The US growth of EV production raised from 25,000 in 2011 to 200,000 EVs in 2015 [39]. The system is still in need of the SL batteries and has not reached saturation yet. However, the expected consequences after the saturation are that the offered SL battery will be less than the needed and consequently low revenue to the owners of the EV and discourage to the EV.

Authors in [41] suggested the grid-connected EV batteries in order to decrease the congestion of the system; as the saturation of such application based on the aggregation of the minimum and maximum capacities that will invade the market by 2063. This solution is expected to be a brilliant estimation if the batteries technologies laboratories did not come up to a proper solution for the battery cost by 2063. In [42], it was predicted that by 2038 the expected power out of the SL batteries would be 584 GWh which could assist about 156 million rural households.

Overall, the penetration of the SL batteries to the market might be achievable by reaching the mass market penetration on certain applications. However, another application which is based on adding a significant amount of batteries is sustained up until now due to the limited amount of SL batteries. Some of the most profitable applications are reserved for other technology as the SL batteries are still weak to invade. As a conclusion, all of these studies should be introduced as a preliminary approach; as the production of the EV is highly unpredictable.

2.3.3.4 Minimize the Upfront Cost of the EV Batteries

As previously mentioned the main impetus of the SL batteries is the increment of the salvage value of the electric vehicles batteries. A study proposed in [43] stated that the salvage value of the EV battery may decrease the monthly battery lease payment from 11% up to 24%. On the other hand, another study presented in [40] handled the problem from a different perspective by assessing the failure rate of the SL batteries. In this study, the refurbishment cost increased, and the salvage value dropped to a range from 6% to 26%.

It is concluded from this section that the contribution of the salvage value in reducing the upfront cost of the EV battery is not enough to encourage the idea of adopting the EV based on this Idea, and consequently it would be better to have a scientific solution to enhance the energy density of the EV battery and use materials that decreases the upfront costs.

2.3.3.5 Early Retirement of the EV Battery and Its Profitability

In spite of the fact that the manufacturers determined specifications below which the EV battery is no more convenient for the automotive life, some studies were performed to test the early retirement on the EV batteries. These studies were aiming to elevate the salvage value of the EV battery and enhance the performance of the SL batteries. These studies were made with two different assumptions. First, there is no refurbishment cost after retirement from the automotive life. Second, the study considered the second life customer acceptance factor. In both cases, the results indicate that the more the EV last in the automotive life the more profitable impacts. However, there are a threshold specs above which a high deterioration rate will occur in the EV battery and then it is no more fitting for this application [39], [44].

The proper linkage between economic and technical viability relies on the aging among the first and second lives, and the proper definition of each. The definition of the end of the automotive life is called first life end of life (FL-EOL). In addition, the maximum level of battery aging in the second life at which the threshold occurs is called second life end of life (SL-EOL).

Finally, the battery performance while aging is an important study that needs decades to be executed; because of the fact that the EV battery performance is dependent on various parameters, such as the rate of discharge, the depth of discharge, and the number of complete discharges among the lifetime. Which is dependent on the owner behavior. The probabilistic models are most fitting in this case. However, it would need a high budget and a long time to be performed. The proper question now is what the viability of the SL batteries is, and if there is invasion would it be prominent. This is discussed in the following section [39], [44].

2.3.4 Technical Viability of SL Batteries

In this section, the analysis of the suitability of the SL batteries for operating on certain applications is carried. In addition, SL batteries performance, power, and energy capabilities are evaluated. Moreover, different modeling techniques and the estimation for the end of life (EOL) is discussed.

2.3.4.1 Technical viability from Applications Perspective

The sizing of the SL battery is little more complicated than the brand new due to the fact that the SL batteries require a relation between the number of cycles and the EOL. In [45], the application of the area regulation was carried; no major issues were recorded among the power and energy assessment. However, it was recognized that under high rate of cycles; 72 cycles/day two – three of the cells should be replaced. In addition, among the time horizon, two to three replacements are needed among 15 years of operation.

The microgrid application was studied in [46], [47]. A multi-objective problem was carried, that indicated frequency regulation, ancillary services for local grid operator management while considering the time of use (TOU) and offering demand charge management for the customer. Based on the results, the SL batteries not only provided peak shaving of renewables DG at a reasonable price, but it also improved the voltage profile of the grid even with increasing the load factor. Moreover, it was recognized while applying SL batteries in the applications of the energy management services in distribution network [48], [49], [50]-[52] that the performance is acceptable. However, the heterogeneity between cells and the reduction in the density from that indicated in the first life batteries is indicated. Which is normal after the batteries are subjected to harsh circumstances such as those in the automotive applications. However, it could be ignored with the larger sizes of the SL batteries.

There are challenges that encounter some of the researches concerning optimal sizing of the SL batteries; because of the few data presented in the literature in this field. However, such studies could be considered as a compact topic that may cover the idea of SL battery as it considers the aging and the profitability of the SL batteries. A study presented in [53] considered the operation of SL batteries to assist the generation of the PV array; based on the system requirements the battery was in operation for 292 days on different locations in the US. The size of the PV and the SL batteries were evaluated. The aforementioned study is an extended work that was done in [54] in which the integration of PV with SL batteries for residential purposes was evaluated. The study aim was to manage the energy of building at the most profitable revenue. The results showed an enhancement in the energy storage capabilities which might reduce the system peaks up to 70 % during summer with less than 5% energy delivered to the grid.

After studying the applications of the SL batteries in the grid; it was concluded that the SL batteries can assist the renewables on different applications the electric power grid; inside a building; in microgrid assistance, on the distribution level or in assisting the transmission level maintaining the ancillary services. In spite of the uncertainty of the SL batteries reliability; the practical applications did not show a huge drawback with respect to the cost difference between the new and SL batteries. In the other side, the SL batteries contribute to the encouragement of adopting more renewables in the system with higher benefits. Moreover, the SL batteries can contribute to utility applications such as voltage regulation with minimal cost compared with alternative technologies.

2.3.4.2 Technical viability from battery perspective

Based on the previous studies [55]-[62], [53], the certain age of the SL batteries is still vague. While the applicability of any of the technical or economic applications is mainly based on battery degradation behavior. The most common observation is the unequal degradation of the batteries among the lifetime. Some of the studies applied the evolution of the Peukert number, which is a method evaluating the degradation of the battery cells with the rate of discharge, round trip, and the internal resistance of the batteries. But none of them showed a certain reason in the unequal capacity fade of the cells. Other studies took over the determination of the number of cycles in the SL batteries with different DOD and different temperatures; before the batteries reach SL-EOL, and it showed a large spectrum in the number of cycles, in the second life, of SL batteries based on the type of the used batteries. However, it is mentionable that the Li-Ion based batteries show the highest number of cycles among the other types. On the other hand, some studies discussed the hazardous effects that might happen if the aging exceeded the threshold knee. The studies indicate that the applications are not possible after the knee threshold of the batteries. Which emphasizes the manufacturer stated specs of the EV battery.

An interesting study that introduced an evaluation technique that is based on the diffusion coefficient and the remaining capacity in the evaluation of the SL batteries, this study gives an indication to the long term second life prediction. However, this study is not practical as it requires the disassembly of the battery components. Moreover, verification techniques carried out on the battery through the first year after retirement to indicate which is eligible and which is not during the second life batteries based on the deterioration rate and the variation in densities.

2.3.4.3 First Life End of Life Criteria for EV Battery Retirement [63]-[65]

In this sector of the literature, the focus is directed to the validity of the assumptions that the EV batteries should be retired after 70-80% of its capacity remaining as well as the power capability. Moreover, the criteria used in the first life end of life (FL-EOL) threshold. EV battery FL-EOL was first defined by USABC in 1996. It was mentionable that the battery should retire after reaching 80% from its initial capacity. However, the studies were carried on the Nickel batteries. Meanwhile, there are numerous studies were carried indicating the maximum allowable capacity fading for the Li-ion batteries and it showed that the Li-ion based batteries might attain a good performance for the automotive life at capacity equals to 70%. Hence, in the literature, it is important to link the model of the battery and the duration of the research to the most recent applications.

The determination of the FL-EOL is based on the rate of discharge and the DOD as mentioned in the previous sections. The aforementioned parameters are based on the owner and the type of ownership. It might follow any of the following three Battery ownership models (BOM):

1. The EV owner is the battery owner.
2. The EV manufacturer is the battery owner, and the EV owner has a leasing agreement for the batteries.
3. A third-party is the battery owner and the EV owner has a leasing agreement for batteries.

In the second and the third scenarios the battery retirement could obey rules; based on the retirement specifications or on the warranty. This will lead to a large number of EV retired batteries at the same time with approximately relatively close state of health (SOH) as it is correlated to the kilometers driven by the car. This duration may vary from 10-12 years for a required replacement.

It could be concluded from the studies that the variable SOH level at the FL-EOL might affect the assessment of the SL batteries. However, monitoring the first life battery through the ownership model control (BOM) will add an extra background on the behavior of the battery in the first life and offer a better chance for assessment at the start of the second life.

2.3.4.4 SL Batteries Modeling Based on the Lifetime

The modeling of the SL batteries is based on the behavior of the EV batteries [44], [66]-[68]; hence, it is characterized by high uncertainty. The model is for the percentage capacity fading along the second life period and determining the threshold deterioration rate beyond which the capacity is no more effective, and the battery should be recycled. There are many parameters that should be considered during this model such as the state of health the average depth of discharge based on the manufacturer recommendation, the average number with complete discharge (up to 100%), the state of health, the C- rate, and the temperature. However, in order to build a model that has a distribution probability function the monitoring should cost time and money to be performed on different EV batteries. On the other side, the modeling of the SL batteries does not require the monitoring of the temperature as it is almost constant. Moreover, based on the literature it was recognized that the deterioration rate of the capacity in the second life is more than that in the first life. This is because of the fact that there are higher lithium losses than when was at the automotive application. The capacity fade is multiplied then by 3.3% than that of the first life. Among the modeling, the deterioration either modeled by a straight line or by an exponential function.in order to describe the deterioration rate of different types of Li-ion batteries. Both are empirical functions and need laboratory readings to emphasize them and put them into reality. Hence, as it was proposed the utilization of the probability distribution functions based on the performance every year and based on the correlation to different parameters is the most promising and expensive as well model.

2.4 Summary

ESS over the decades had different forms based on the kind of energy stored inside. The most important parameters that affect the decision of using a certain type of ESS are the energy density, the power density, the self-discharge rate, the efficiency, and the field of the project. Most of the ESS could find an appropriate application on the transmission level; this returns to the importance of the ESS in the market, TOU, reducing the system congestions, and might control the electricity prices. On the other hand, the profitability to the capacity ratio makes most of ESS deviate from the distribution level applications. However, the controller of this decision is economic benefits. There is no doubt that the most appropriate ESS for distribution system applications is batteries with its different types; this is because of the capacity flexibility and high efficiency. However, the high cost of the BESS may form a drawback; that may lead to discouragement to the customers or small investors in the distribution system to adopt batteries in their projects. In addition, the healthy environmental impact of the BESS if integrated with renewables, in the distribution network, made the governments encourage the usage of some projects such as net-zero metering and building energy efficiency management.

On the other hand, it was recognized that obstacle that affect the growth of the EV technology is the cost of the batteries. This made the researches directed to find a solution to this problem. One of the solutions is to give the EV batteries a second life in the electric grid power applications. Many studies dealt with different perspectives; economically, study the viability, the market response, and it was tested in different applications. The target of these studies is to maximize the salvage value keeping into consideration the incentives to the second life users to adopt this idea instead of new batteries.

The SL batteries have some drawbacks; the most prominent is the uncertainty of the state of health of them; the annual capacity fade, and the SL-EOL. It was discussed that the performance of the EV batteries in the first life affects second life applications. The performance could be controllable in case of battery ownership model control (BOM); the controllable scenario is when the batteries are leased by a third party or by the manufacturer. In this case, the state of health is controllable along the lifetime of the first life. However, many studies were carried out in different grid applications and it was noticed that the power and energy performance were good. However, the heterogeneous performance of some cells among the others of the battery back was recognized.

It could be concluded that the SL batteries have some drawbacks; however, these drawbacks will not affect the grid needs if the cost is a factor in the study. The SL batteries might encourage investments in the distribution system, which was economically discouraged in previous times.

Chapter 3

Integration of Photovoltaic Distributed Generators with the Distribution System

3.1 Introduction

The target of this study is to evaluate the economic worth of the Second Life SL battery in the distribution grid applications. The application selected in this thesis is to utilize the SL battery to assist the PVDG so as to maximize the economic benefits of the PVDG project. In order to execute the aforementioned objective, two stages are considered. First, economic study is performed on PVDG alone then PVDG with SL battery. Moreover, to build up the system and check the constraints; load flow is performed considering the annual growth of the load. The target of the load flow is to determine the Maximum Allowable Injected Power (MAIP) that keeps the bus voltage and the reverse power to the substation within the limits set by the utility. In addition, a load forecasting technique is developed; in which the growth of the load along the project lifetime is considered; the forecasting technique is able to determine the minimal loading considering the typical day model of each season. Meanwhile, in order to integrate the PV DG a model was developed; which considers the stochastic nature of the PV DG a probabilistic model was developed which the gives the most likelihood output power per seasonal hours.

The General objective of the work presented in this chapter is to select the suitable capacity of the photovoltaic DG to be connected with the distribution feeder. The rationale of the selection procedure is to determine the best DG size, among the candidate sizes, that maximizes the net present value of the DG investment project and maintain the distribution system technical constraints. In the presented analysis, it is assumed that the DG rated capacity may exceed the maximum allowable injected power (MAIP) at the DG bus. However, in this case, the utility will curtail the extra DG power that exceeds the maximum allowable value.

The DG investor has two choices; the first is to connect as small size DG less than the MAIP power and the second choice is to connect a large size DG and allow the utility to perform the adequate curtailment. On the other hand, the MAIP is assumed to be a value that is determined by the utility at each bus. In case the DG power exceeded this value, the technical constraints (i.e. the voltage limits and the reverse power constraint) would be violated.

The maximum power value varies as the forecasted load changes; e.g. if the forecasted load at a certain year is larger than the base year load, the maximum allowable power injection MAIP will increase in return. Thus, a long-term forecasting technique is required to determine the forecasted load and the corresponding MAIP along the DG project life time. These forecasted values will give the DG investor a boarder view in order to select the most appropriate DG capacity.

In this chapter, a load forecasting technique is presented to determine the forecasted load during the life time of the DG project. Moreover, a strategy is presented for probabilistic modeling of photovoltaic DG power considering the stochastic nature of solar irradiances. The results of the load forecasting technique and the modeling strategy are integrated with a load flow study in order to determine the maximum allowable power injection MAIP along the project life time. Finally, based on the obtained results, the best DG size is selected from the candidates' sizes. The criterion of selection is based on the maximization of the net present value of the DG investment profit.

3.2 Load Forecasting

Load forecasting is a vital tool in the majority of power system studies. For reliable solution of the design, planning, operational planning, and operation problems, accurate load forecasting technique should be utilized first. Precise load forecasting helps the electric utility to make unit commitment decisions, reduce spinning reserve capacity and schedule device maintenance plan properly. Moreover, system demand prediction is a significant feature in the developments of power system models due to the modern deregulated electricity markets [69].

Precise load forecasting is a challenging problem as electric loads are characterized by high unpredictable characteristics. However, the loads are strongly correlated to the weather conditions, season, time and geography [70]. Thus, load forecasting technique should consider the stochastic pattern of the loads as well as other correlated factors.

From the perspective of the time horizon, load forecasting technique could be categorized into four main categories; the very short term, the short-term, the medium-term, and the long-term load forecasting. A brief summary of the four categories and the corresponding applications of each are introduced in Table 3-1 [71]-[72].

Table 3-1 Classification of Load Forecasting According to Time Horizon

Forecasting horizon	Time scale	Application
Very short-term	few minutes to an hour ahead	• Power system frequency control • Energy purchasing • Demand side management
Short-term	from one hour to one week	• Economic dispatch • Reserve requirement • Day-ahead electricity market • unit commitment • Demand side management
Medium-term	One week to one year	• Planning of future needs for expansion, equipment purchases, or staff hiring. • Energy purchasing
Long-term	longer than one year	• scheduling fuel supplies and unit maintenance • Financial planning

The system demand is highly correlated with the meteorological /seasonal conditions. Thus, the network planners are in need of a load forecasting technique that is capable of considering the stochastic nature of the electric system demand and the meteorological/seasonal conditions.

In this section, a novel Copula based approach is proposed for load forecasting. This approach takes into account the stochastic nature of the electric loads by determining the most adequate cumulative distribution functions (CDFs) from the available historical data of the loads. Moreover, the effects of the meteorological conditions on accurate forecasting are taken into consideration by dividing the available data based on a seasonal/hourly/nature classification. The introduced approach employs Monte-Carlo simulation MCS in conjunction with Gaussian Copula method for considering the stochastic dependence between different time segments of the forecasted load.

3.2.1 The Proposed Forecasting Technique

In order to obtain the annual MAIP that keeps the bus voltages and the reverse power within the preset utility limits the worst case loading is considered in the planning problem .Thus, the load forecasting technique should be able to determine the annual mimimum loading, which is considered to be the minimum annual load, taking into consideration the annual load growth. The proposed load forecasting technique consists of two main stages. First, is to forecast the load variation trend. The second stage aims to determine the typical day model, for each of the four seasons, for the base year. Based on the trend forecast and the base year typical day model, the typical day models for the forecasted years could be obtained.

A. Load Variation Trend

In order to determine the trend for the load variation over the forecasted period the following algorithm is proposed;

1. Divide the available historical load data based on seasonal/annual classification. Firstly, the available data is classified based on the year (each year data is separated). Secondly, each year data is separated again based on the season. Thus, the total number of datasets is equal to 4 N (N historical years X 4 seasons).

2. Determine the CDF corresponding to each dataset separately based on the available data in this dataset $((F_{w1}, F_{w2}, \ldots . F_{wN}), (F_{sp1}, F_{sp2}, \ldots . F_{spN}), (F_{S1}, F_{S2}, \ldots . F_{SN}), (F_{f1}, F_{f2}, \ldots . F_{fN}))$ where $(F_{wN}, F_{spN}, F_{SN}, F_{fN})$ are the CDFs of year N for winter, spring, summer and fall. Gaussian CDF is selected for simulating the random behavior of the load.

3. For the winter season datasets (N datasets), determine the rank correlation between the CDFs of each dataset and the CDF of the first-year dataset; i.e. $\rho_{n,1}$.
4. Generate (N) independent uniformly distributed random numbers $(u_{1,} u_2 \ldots \ldots \ldots . . u_N)$
5. Convert the independent random numbers to correlated uniform random numbers $(u_{c1,} u_{c2} \ldots \ldots \ldots . . u_{cN})$ using the Gaussian- Copula method and the calculated rank correlation using (3.1).

$$
\begin{aligned}
u_{c1} &= u_1 \\
u_{cn} &= C^{-1}_{V|U}(u_n | u_1, \rho_{n,1})
\end{aligned}
\tag{3.1}
$$

6. For each random number, the inverse of the corresponding CDF $(F_{w1}^{-1}(u_{c1}), F_{w2}^{-1}(u_{c2}), \ldots . F_{wN}^{-1}(u_{cN)})$ is used to determine the load at the current simulation (i) $(L_{W1}^i, \ldots . . L_{WN}^i)$
7. Repeat the Monte Carlo Simulations, for very high number, to obtain the most likely load for the winter season for each year. The dynamic average is calculated using (3.2)

$$L_{wn}^{ave} = \frac{1}{mc}\sum_{i=1}^{mc} L_{wn}^{i} \tag{3.2}$$

Where: L_{wn}^{ave} the expected value of the load for winter season at year n and mc is the total number of MCS.

8. Determine the linear equation that fits the obtained expected average loads at the N years and use this equation to forecast the expected loads for each year over the period of the study.

9. Repeat steps 3-8 for the other seasons.

B. Typical Day Model

In order to determine the typical day model (i.e. 24 values of the expected load representing the 24 hours of the day) for the four seasons for the base year, the following algorithm is proposed;

1. To remove the effect of the trend, the available historical data (for each season for each year) is divided by the corresponding most likely value of the season and the year (obtained from the previous algorithm).

2. Divide the trend-free load data based on seasonal/hourly classification. Firstly, the available data is classified based on the season (each year data is separated). Secondly, each season data is separated again based on the hours. Thus, the total number of datasets is equal to 96 (*24* hours X 4 seasons).

3. Determine the CDF corresponding to each dataset separately based on the available data in this dataset. Gaussian CDF is selected for simulating the random behavior of the load.

4. For a dataset, generate *mc* (very high number enough for MCS convergence) independent uniformly distributed random numbers.

5. Determine the load corresponding to each random number from the inverse of the CDF of the dataset.

6. Determine the most expected load for the dataset (the average of *mc* random loads obtained from the MCS)

7. Repeat steps 3-6 for the other datasets to determine the most expected load at all seasons at all hours.

3.2.2 Results of the Forecasting Technique

The load forecasting technique presented in section 3.2.1 is applied to a 7 years of historical load data collected in Canada from 2012 to 2018. The obtained results are discussed as follows;

C. Results for the Load Trend

The available historical data is separated to 28 datasets (4 seasons X 7 years) and the Gaussian CDF is obtained for each dataset. The rank correlations are obtained between the CDF of the year 2012 and the remaining years CDFs for each season.

The expected load values for each dataset is obtained using the algorithm described in section 3.2.1, A. Moreover, the trend equation that fits the obtained loads is determined for each season; a sample of the trend equation for the winter season is presented in Figure 3.1. The trend equations are used for forecasting the expected load for each season over the period of the study (i.e. 20 years from 2019 to 2038). The complete results for the forecasted loads as ratio to the most likely load of the base year (2018) are presented in Figure 3.2 to Figure 3.5.

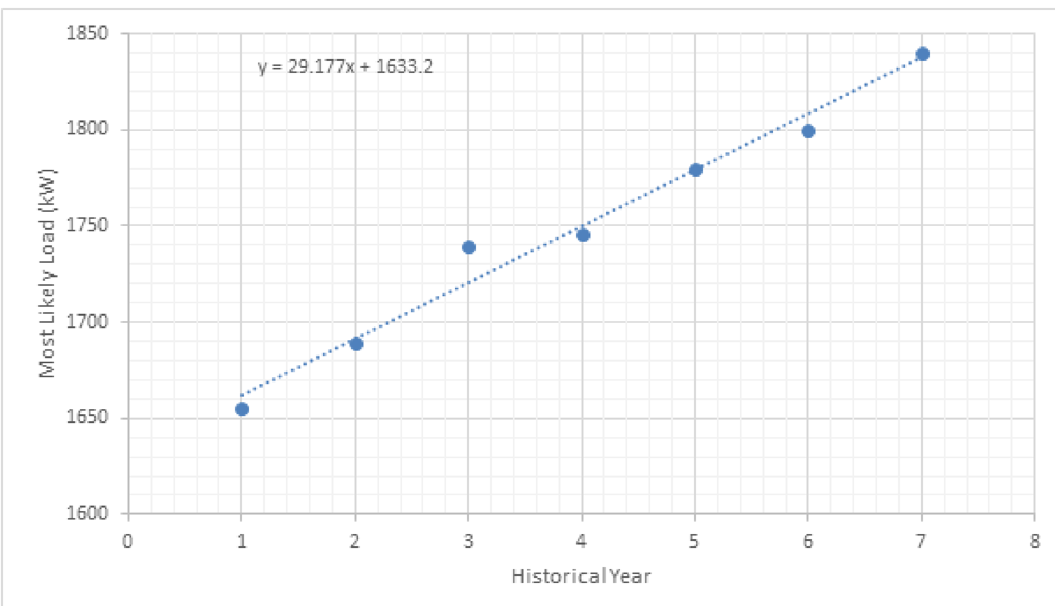

Figure 3.1 Trend Equation for Winter Season

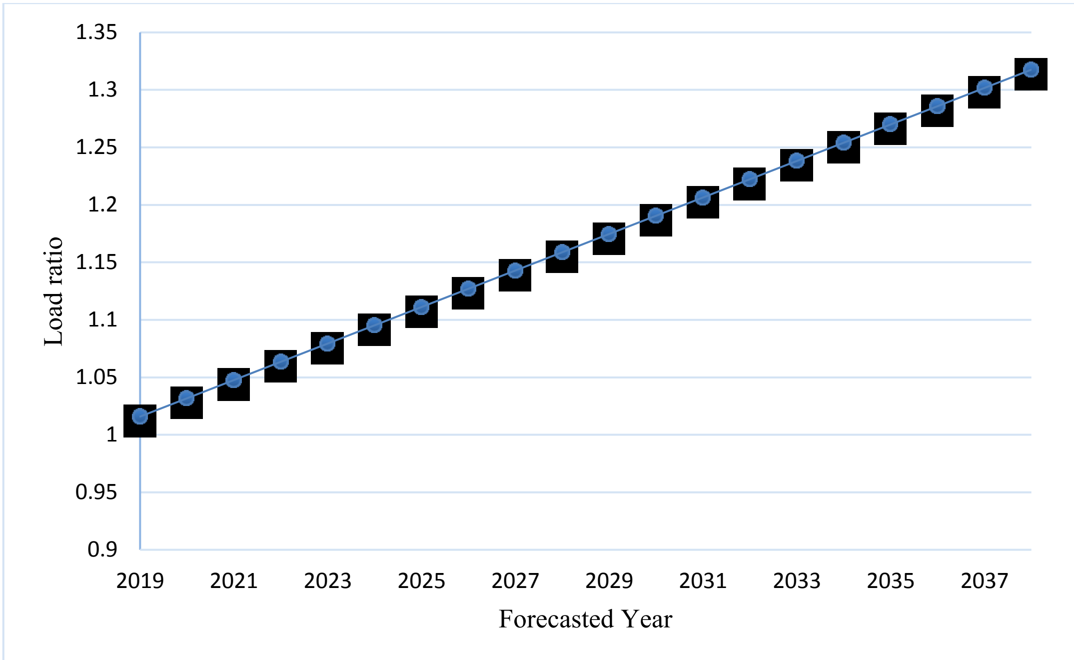

Figure 3.2 Trend Forecast for Winter Season

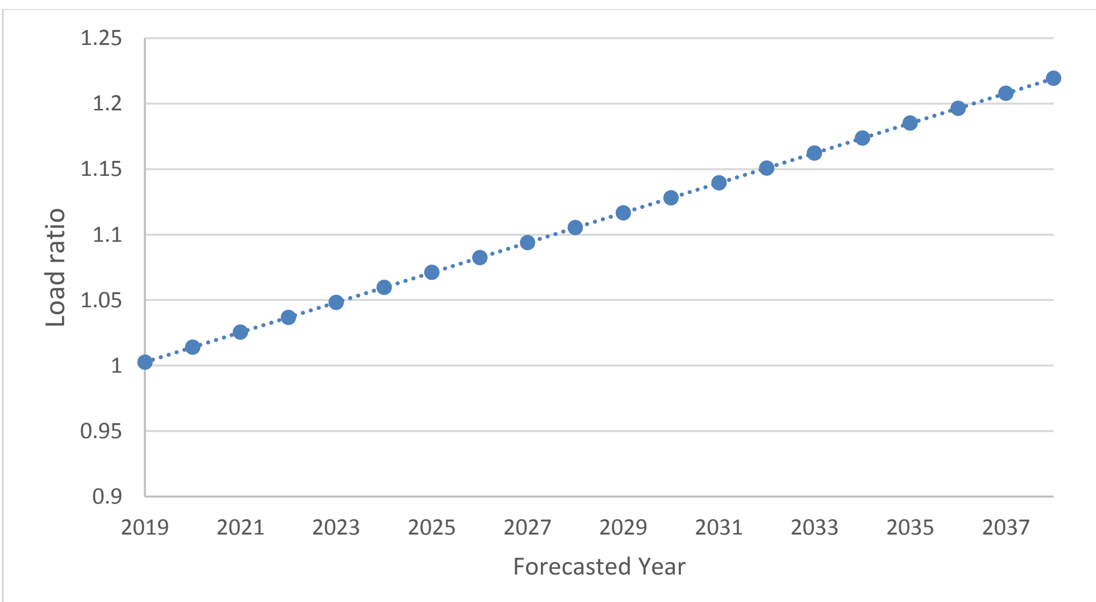

Figure 3.3 Trend Forecast for Spring Season

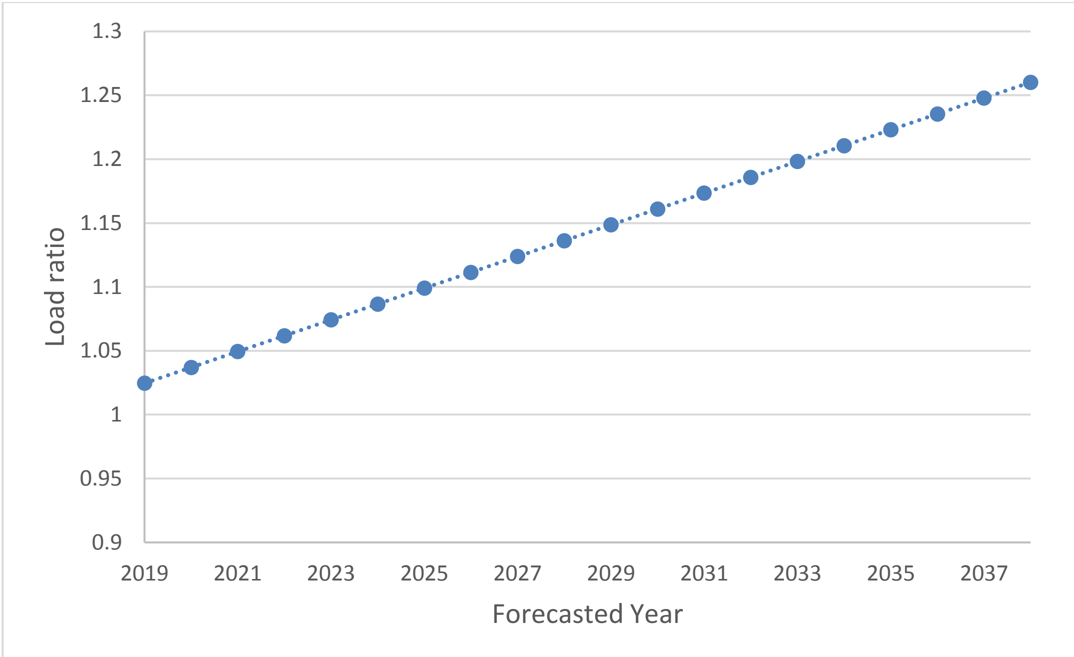

Figure 3.4 Trend Forecast for Summer Season

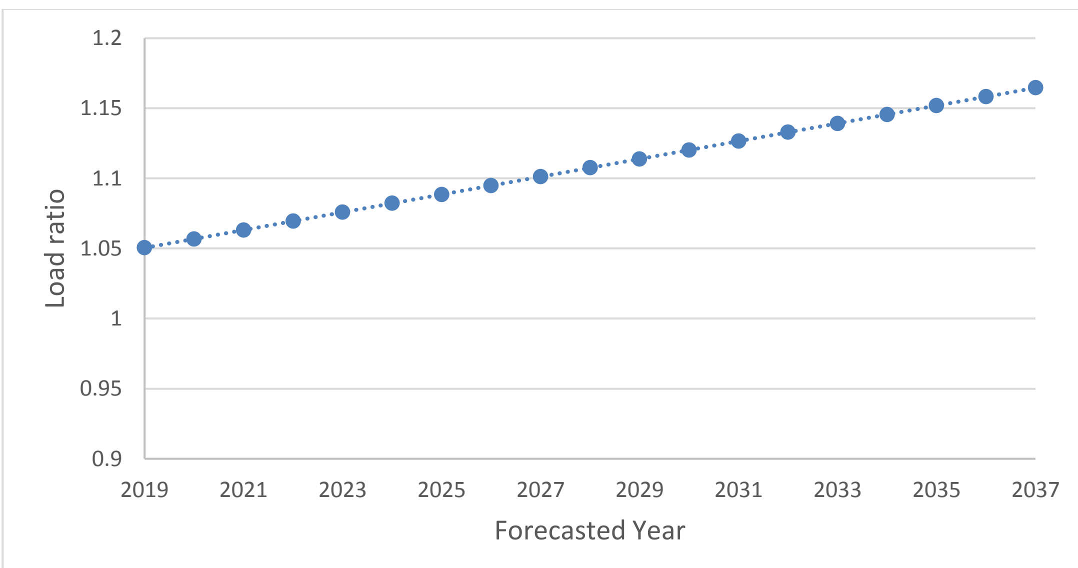

Figure 3.5 Trend Forecast for Fall Season

A. Typical Day Model for the Base Year

The available historical data is firstly divided by the corresponding most likely load values for each year for season and then separated to 96 datasets (4 seasons X 24 hours) and the Gaussian CDF is obtained for each dataset. The algorithm presented in section 3.2.1, B is applied to determine the expected typical day model for each season for the base year (2018). The obtained hourly results (the 96 values) are then divided by the maximum value of the 96 hours to determine the normalized typical day model for the four seasons. The normalized typical day models are presented in Figure 3.6.

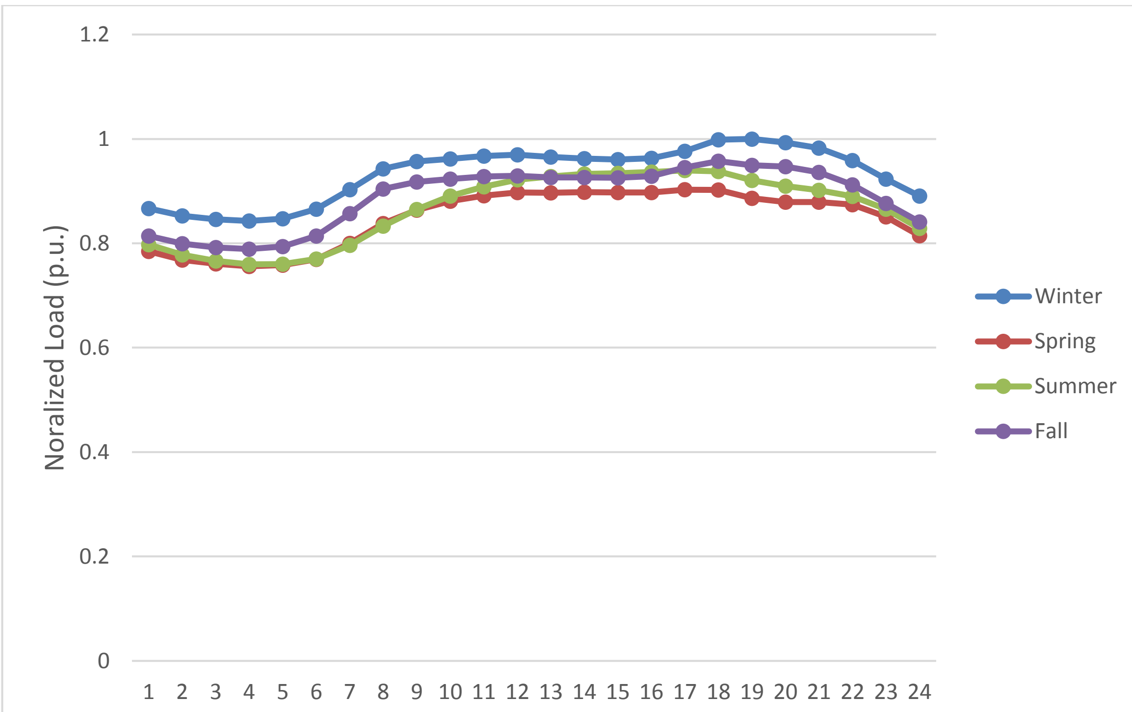

Figure.3.6 Typical Day Model for the Four Seasons

B. Typical Day Model for the forecasted Years

The results obtained from sections *A* and *B* are used to determine the typical day models for the forecasted years. The ratios obtained in section A are multiplied by the typical day models of the base year; to determine the forecasted typical day models over the period of the study. A sample of the results (the forecasted day models for the last forecasted year; 2038) are presented in Figure 3.7.

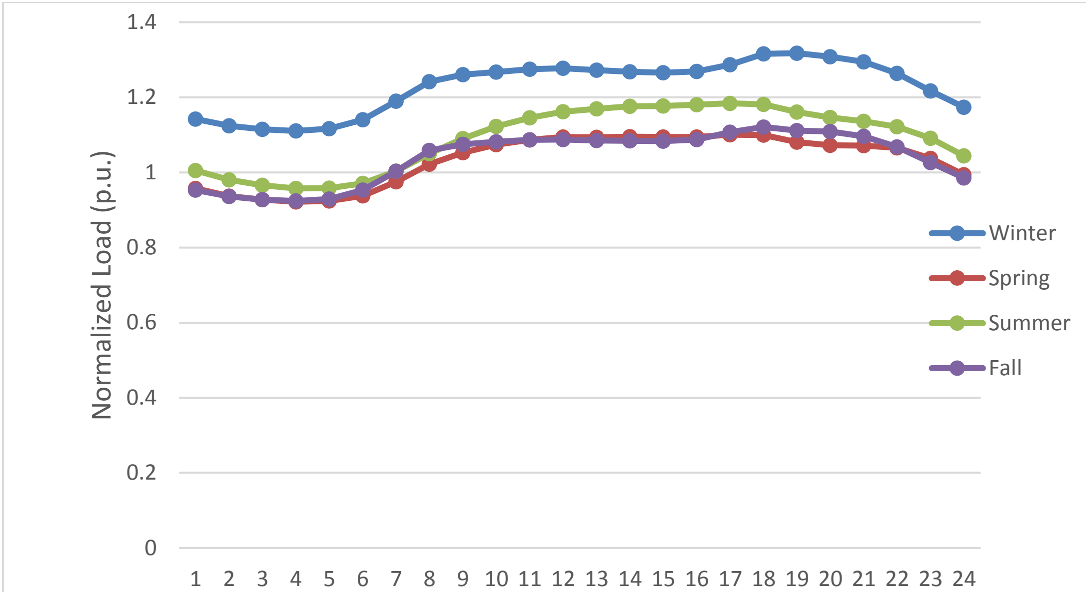

Figure 3.7 Forecasted Day Model for year 2038

3.3 Photovoltaic DG Modeling

3.3.1 The Proposed PV DG Modeling Technique

A similar algorithm to that presented in section 3.2.1, B is used to determine the most probable output power from the PV DG. The PV DG modeling algorithm is discussed as follows;

1. Divide the available historical solar irradiances data based on seasonal/hourly classification. Firstly, the available data is classified based on the season (each year data is separated). Secondly, each season data is separated again based on the hours. Thus, the total number of datasets is equal to 96 (*24* hours X 4 seasons).
2. Determine the CDF corresponding to each dataset separately based on the available data in this dataset. Beta CDF is selected for simulating the random behavior of the solar irradiance.
3. For a dataset, generate mc (very high number enough for MCS convergence) independent uniformly distributed random numbers.
4. Determine the simulated solar irradiance corresponding to each random number from the inverse of the CDF of the dataset.

5. Calculate the corresponding PV DG power corresponding to each simulated solar irradiance obtained from the previous steps using (3.3 – 3.7) [73]

$$T_c = T_a + S_a(\frac{N_{OT} - 20}{0.8}) \tag{3.3}$$

$$I = S_a[I_{sc} + K_i(T_c - 25)] \tag{3.4}$$

$$V = V_{oc} - K_v \times T_c \tag{3.5}$$

$$FF = \frac{V_{MPP} \times I_{MPP}}{V_{oc} \times I_{sc}} \tag{3.6}$$

$$P_s = N \times FF \times V \times I \tag{3.7}$$

Where

T_c	Cell temperature °C
T_a	Average hourly ambient temperature °C
S_a	Simulated solar irradiance kW/m²
N_{OT}	Nominal operating temperature of cell °C
I	Module current (A)
I_{sc}	Short circuit current (A)
K_i	Current temperature coefficient A/°C
V	Module voltage (V)
V_{oc}	Open-circuit voltage (V)
K_v	Voltage temperature coefficient (V/°C)
FF	Fill factor
V_{MPP}	Voltage at maximum power point (v)
I_{MPP}	Current at maximum power point (A)
P_s	Simulated output power of the PV module
N	The number of modules per array.

6. Determine the most probable PV DG for the dataset (the average of *mc* PV powers obtained from the MCS)
7. Repeat steps 3-6 for the other datasets to determine the most probable PV DG powers for all seasons for all hours.

3.3.2 The Results of the PV Modeling

The algorithm presented in section 3.3.1 is applied to ten years of historical data collected from Ontario, Canada during the period 2009 – 2018. Table 3-2 presents the values of the constants and parameters required to calculate the PV output per module. The 24 hours PV module converged powers for the four seasons are presented in Fig 3-8 (for a 10 kW DG consists from 40 modules).

Table 3-2 characteristics of the PV module [74]

Module characteristics	Features
Watt peak (W)	250
Open circuit voltage (V)	37.1
Short circuit current (A)	8.91
Voltage at maximum power (V)	29.8
Current at maximum power (A)	8.39
Voltage temperature Coefficient (mV/°C)	132
Current temperature Coefficient (A/°C)	5.52
Nominal cell operating temperature (°C)	46

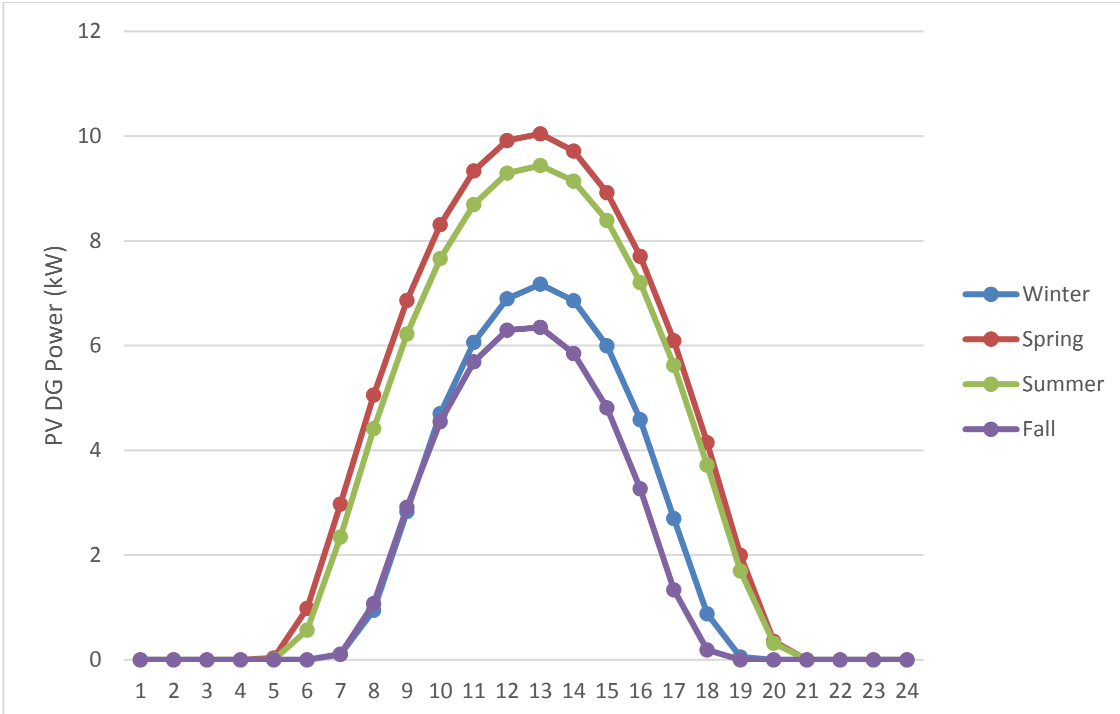

Figure.3.8 PV DG Expected Powers

3.4 Maximum Allowable Injected Power

3.4.1 Problem Formulation

In this subsection, the maximum allowable power, that is allowed to be injected at a certain bus, is determined. This allowable power should be determined by the utility in order to maintain the system technical constraints. In addition, this allowable power is to be obtained for each year over the period of study.

The problem is formulated to maximize the DG penetration at a certain bus #*j* for a certain year *y*:

$$\max P_{inj}(j, y) \tag{3.8}$$

Subjected to the following technical constraints:

- Substation reverse power: the reverse power at the substation bus is limited to 40 % of the substation power.
- Voltage limits: all voltages for all system buses are constrained as follows;

$$V_{\min} \le V_i \le V_{\max} \tag{3.9}$$

In the presented analysis it was assumed that the DGs are allowed to connect to a certain bus of the feeder determined by the utility. Moreover, it is assumed that the loading condition is set to the minimum loading condition for each year; i.e. the minimum loading for a year is used to determine the maximum allowable power at this year; since the modeling is based on the worst case scenario.

3.4.2 Results

The problem formulated in section 3.4.1 is solved using MATLAB and tested on the IEEE 33 bus test feeder shown in Figure 3.9. It was assumed that DGs are allowed to connect to bus number 32 only. The minimum loading condition in each year is used to determine the maximum allowable injected power. The minimum loading ratios for all years over the period of study are presented in Table 3-3; the loading ratio, for a certain year, is multiplied times the original loading of all buses of the IEEE 33 bus system to simulate the minimum loading conditions for this year. The maximum allowable injected powers for the period of study are determined and presented in Table 3-4.

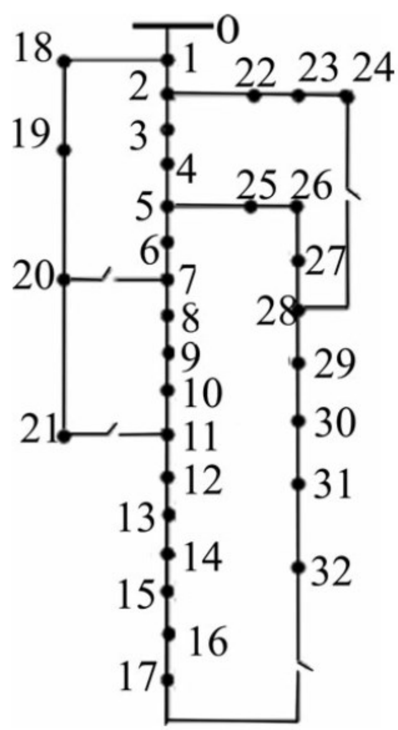

Figure 3.9 Layout of the 33-bus feeder.

Table 3-3 Minimum Loading Ratio Over the Study Period

Year	Minimum Loading Ratio (p.u.)
2019	0.758051
2020	0.76667
2021	0.77529
2022	0.783909
2023	0.792528
2024	0.801148
2025	0.809767
2026	0.818387
2027	0.827006
2028	0.835625
2029	0.844245
2030	0.852864
2031	0.861483
2032	0.870103
2033	0.878722
2034	0.887342
2035	0.895961
2036	0.90458
2037	0.9132
2038	0.921819

Table 3-4 Maximum Allowable Power Results

Year	Maximum Allowable Injected Power (kW)
2019	700.9
2020	710.8
2021	721.4
2022	729.2
2023	730.5
2024	738.2
2025	746.4
2026	751.6
2027	768.8
2028	774.1
2029	785.3
2030	790.5
2031	804.3
2032	812.2
2033	814.1
2034	819.5
2035	828.7
2036	840.3
2037	846.1
2038	854.7

3.5 Selection of DG size based on the profitability

In this section, the most profitable DG size is selected in order to maximize the DG investment project. In this selection algorithm, it was assumed the DG is connected to a certain bus of the distribution system (i.e. bus 32) without any energy storage. Also, it was assumed that the utility will curtail the portion of DG power greater than the maximum allowable injected power calculated from section 3.4. Since the maximum allowable injected power is increasing over the forecasted period (the project life time), the amount of active power curtailed from PV DG will decrease all over the project life.

As shown in the demonstrative example presented in Figure 3.10, for a DG capacity of 1 MW, for the first year of the DG project life the curtailment will be any DG power greater than 700.9 kVA. The curtailed power will decrease all over the project life and the active power curtailment for the 20th year will be 854.7 kVA. This means if the DG size is 700 kW, no curtailment will occur during the project lifetime. Also, if the DG size is 800 kW, active curtailment will occur for the years 2019-2030 and no curtailment will occur for the remaining years. Thus, the DG investor should select the optimal DG size that maximizes the net present value of the DG project investment taking the potential active power curtailments into account.

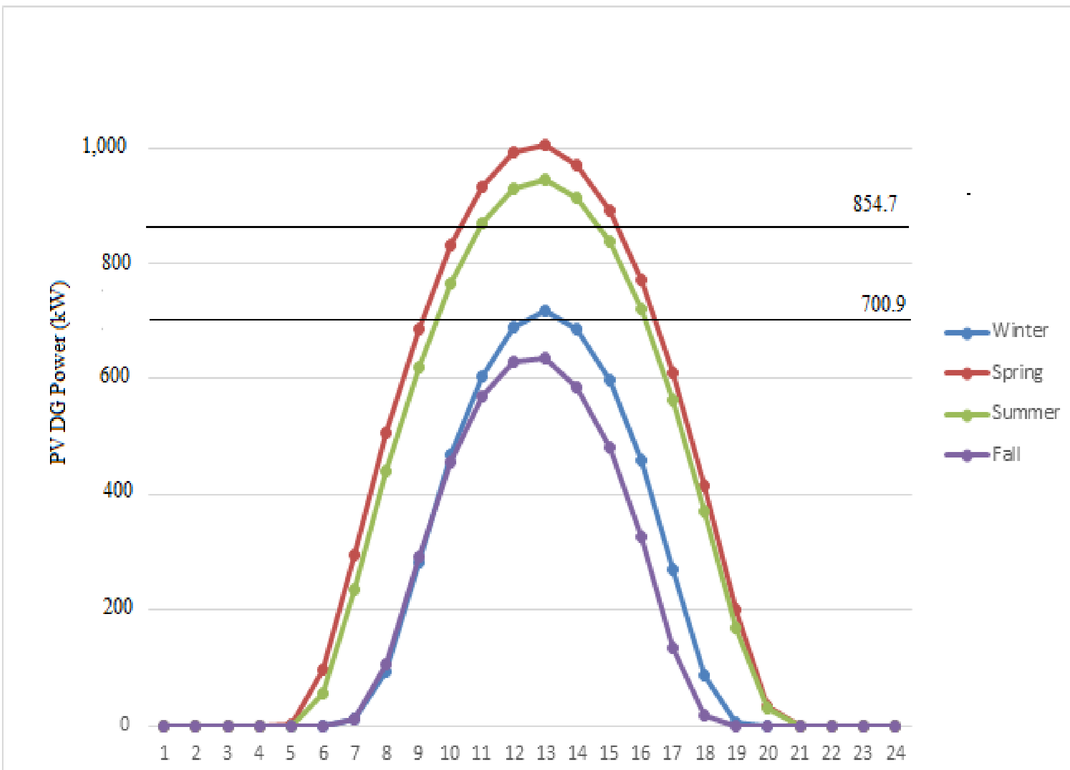

Figure 3.10 Impact of the Active Power Curtailment

3.5.1 Economic Evaluation of the DG Project

In order to calculate the NPV of the DG project, the after-tax cash flow, presented in [73], is performed. This cash flow considers the inflation rate, the escalation rate, the taxes, the depreciation rate, and the capital cost allowance. The after-tax cash flow algorithm is discussed as follows;

1. Calculate the DG capital cost (CAP) using (3.10) [73]

$$CAP = P_{DG}^{rated} \times (Per\,unit\,capital\,\mathrm{cost}) \tag{3.10}$$

2. Calculate the income per year for the project lifetime. [73]

$$Income(y) = 91 \times (1 + \mathrm{esc}\%)^{y-1} \times \sum_{S=1}^{4} \sum_{hr=1}^{24} [P_{DG}(S,hr) \times \Pr(S,hr)] \tag{3.11}$$

Where $Income(y)$ is the DG project income for certain year (y), $P_{DG}(S,hr)$ is the DG generated power (energy as the power is assumed constant over the hour) at certain hour (hr) at certain season (S) for certain year, $\Pr(S,hr)$ is the energy prices at certain season and hour, esc is the escalation rate of the feed-in-tariffs, and 91 represents the number of days per season.

3. Calculate the capital cost allowance (CCA) per year, for each year of the project life time, using (3.12) [73]

$$CCA(y) = dep(y) \times [\ CAP - \sum_{j=0}^{y-1} CCA(j)] \tag{3.12}$$

   Where $dep(y)$ is the depreciation rate at a certain year (y).

4. The CCA is used for taxes calculation; the taxes for each year are determined using (3.13) [73]

$$Taxes(y) = (Income(y) - CCA(y)) \times Tax\,rate(y) \tag{3.13}$$

5. Calculate the inflation adjusted after tax cash flow ($C(y)$) for each year using (3.14) [73]

$$C(y) = \frac{Income(y) - Taxes(y)}{(1 + \inf)^{y}} \tag{3.14}$$

   Where inf is the inflation index

6. Calculate the NPV for the DG project using (3.15) [73];

$$NPV = \sum_{y=1}^{N} \frac{C(t)}{(1 + \mathrm{int})^{y}} - CAP \tag{3.15}$$

Where NPV is the net present value, N is the project lifetime, and int is the interest rate.

3.5.2 Maximizing the Profit of DG Project

The method of determining the best DG size; in order to maximize the DG profit, is carried out heuristically by evaluating all possible DG sizes economically. It is assumed that the available DG sizes are multiple of 10 kW and the maximum available DG size is 1000 kW. Thus, the economic evaluation procedure presented in section 3.5.1 is tested for all the available DG sizes between 10 kW and 1000 kW to determine the size that achieves the maximum NPV of the profit. The economic parameters presented in Table 3-5 is used to perform the required economic evaluation. Moreover, the PV DG energy selling prices for two test cases, fixed and variable, are presented in Table 3-6.

Table 3-5 PV DG Parameters [73]

Parameter	Value
DG capital cost	2.8 $/W
DG investment lifetime	20 yr
Escalation percentage	0%
Fixed operation and maintenance cost	10 $/kW. yr
Variable operation and maintenance cost	0
Depreciation rate	20%, 10% for the first year
Corporate tax rate	26 %
Inflation rate	2 %
Interest Rate	3 %

Table 3-6 Selling Prices for PV DG Energy [73]

Test case	PV Energy Selling Prices	Time/season
Case #1: Fixed prices	0.288 $/kWh	for all hours for all seasons
Case #2: Variable prices	0.33 $/kWh for peak hours	(11 am-5 pm for Summer and Spring) (7am-11 am and 5pm-7pm for Winter and Fall)
	0.2375 $/kWh for mid-peak hours	(11 am-5 pm for Winter and Fall) (7am-11 am and 5pm-7pm for Summer and Spring)
	0.1625 $/kWh for off-peak hours	7 pm- 7 am for all seasons

Test Case #1: Fixed Prices

For the fixed prices scenario, the results for the economic evaluation procedure show that the optimal DG size is 1000 kW; i.e. the maximum NPV (3,847,766) occurs at DG size equals to 1000 kW. These results could be explained that increasing the DG size increases the amount of output energy even if the active power curtailment is considered. A sample of the obtained NPVs for the profit for different DG sizes in presented in Table 3-7 . Moreover, the complete after-tax cash flow for the optimal DG size is summarized in Table 3-8. Furthermore, total income reduction (for the 1000 kW DG) due to active power curtailment for each year over the project lifetime is presented in Table 3-9.

Table 3-7 DG Profit for Test Case #1

DG Size (kW)	NPV of the DG profit ($)
600	2,558,405
700	2,984,806
800	3,377,240
900	3,657,516
950	3,762,832
1000	3,847,766

The results presented in Table 3-9 show that the income reduced due to curtailment is decreasing along the project lifetime due to decreasing curtailment. The NPV of the income reduction is 416, 242 $; i.e. 10.82% of the profit NPV.

Table 3-8 After-Tax Cash Flow for the Optimal DG Size for Test Case #1

Year	Income ($)	CCA ($)	Taxes ($)	C(Y)	Present Value ($)
1	641640	280000	94026.4	536876.1	521238.8976
2	645272.4	504000	36730.83	584911.2	551334.8777
3	649125	403200	63940.5	551432.4	504638.7745
4	651782.5	322560	85597.84	523067.1	464738.3287
5	652225.4	258048	102486.1	497915.8	429506.538
6	654848.8	206438.4	116586.7	477961.3	400285.1024
7	657642.6	165150.7	128047.9	461044.1	374871.0092
8	659414.2	132120.6	137096.4	445793.3	351913.341
9	665274.4	105696.5	145490.3	434932.1	333339.2274
10	666865.2	84557.17	151400.1	422860.9	314648.2348
11	670094	67645.73	156636.6	412954.9	298327.3727
12	671593.1	54116.59	160543.9	402958.8	282627.2049
13	675571.5	43293.27	164392.3	395158.1	269083.4409
14	677849	34634.62	167235.7	386981	255840.037
15	678396.7	27707.69	169179.1	378356.1	242852.4133
16	679953.5	22166.15	171024.7	370727	231024.8242
17	682605.7	17732.92	172866.9	364036.4	220247.9816
18	685672	14186.34	174586.3	357841.5	210194.159
19	687040.1	11349.07	175679.7	351013.5	200178.1113
20	689068.6	9079.257	176797.2	344743.9	190876.3646

Table 3-9 Income Reduction Due to Curtailment for Test Case #1

Year	Income Reduction ($) due to active power curtailment
1	66,762
2	63,129
3	59,277
4	56,619
5	56,176
6	53,553
7	50,759
8	48,988
9	43,128
10	41,537
11	38,308
12	36,809
13	32,831
14	30,553
15	30,006
16	28,449
17	25,797
18	22,730
19	21,362
20	19,334

Test Case #2: Variable Prices

For the variable prices' scenario, the optimal DG size is also 1000 kW; i.e. the maximum NPV (3,592,090) occurs at DG size equals to 1000 kW. A sample of the obtained NPVs, for the profit for different DG sizes, is presented in Table 3-10. Moreover, the complete after-tax cash flow for the optimal DG size is summarized in Table 3-11. Furthermore, total income reduction (for the 1000 kW DG) due to active power curtailment for each year over the project lifetime is presented in Table 3-12.

Table 3-10 DG Profit for Test Case #2

DG Size (kW)	NPV of the DG profit ($)
600	2,457,778
700	2,867,407
800	3,234,267
900	3,460,487
950	3,531,755
1000	3,592,090

Table 3-11 After-Tax Cash Flow for the Optimal DG Size for Test Case #2

Year	Income ($)	CCA ($)	Taxes ($)	C(Y)	Present Value ($)
1	612444.4	280000	86435.54	515695	500674.7
2	615946.5	504000	29106.1	564052.7	531673.8
3	619696.3	403200	56289.03	530911.2	485859
4	622455.5	322560	77972.84	503017.8	446924.8
5	622915.4	258048	94865.52	478271	412560.8
6	625639.3	206438.4	108992.2	458767.8	384210.8
7	628540	165150.7	120481.2	442295.8	359626.9
8	630379.5	132120.6	129547.3	427455.5	337437.3
9	636464	105696.5	137999.6	417092.8	319666.9
10	638338.9	84557.17	143983.3	405543.8	301762.7
11	642300.9	67645.73	149410.3	396413.7	286377.7
12	644140.4	54116.59	153406.2	386940.6	271392.3
13	649022.2	43293.27	157489.5	379970.7	258741.6
14	651816.8	34634.62	160467.4	372381.4	246188
15	652488.9	27707.69	162443.1	364111.2	233709.1
16	654399.2	22166.15	164380.6	356952	222440.7
17	657653.7	17732.92	166379.4	350849.7	212269.8
18	661502.6	14186.34	168302.2	345318.9	202838.4
19	663225.2	11349.07	169487.8	338916.6	193279.4
20	665779.4	9079.257	170742	333146	184454.8

The results presented in Table show that the income reduced due to curtailment is decreasing along the project lifetime due to decreasing curtailment. The NPV of the income reduction is 504, 206 $; i.e. 12.3% of the profit NPV. This high reduction in income may encourage the DG investor to connect battery energy storage at the same bus of the DG to reschedule the DG output power in order to minimize the curtailment and maximize the profit as discussed in Chapter (4).

Table 3-12 Income Reduction Due to Curtailment for Test Case #1

Year	Income Reduction ($) due to active power curtailment
1	77,679
2	74,177
3	70,427
4	67,668
5	67,208
6	64,484
7	61,584
8	59,744
9	53,660
10	51,785
11	47,823
12	45,983
13	41,101
14	38,307
15	37,635
16	35,724
17	32,470
18	28,621
19	26,898
20	24,344

3.6 Summary

This chapter presents a novel methodology for optimal integration of PV DGs with the distribution network; while maintaining the distribution system technical constraints. To achieve this objective, four techniques were presented; i.e. long-term load forecasting technique, PV power modeling strategy, determination of the maximum allowable injected power at the potential DG bus, and the selection of the PV DG size for maximizing the DG profit.

The obtained results show that the active power curtailment is causing a NPV reduction of 10.82% of the expected DG income. Thus, the use of battery storage at the same bus of the DG may positively affect the NPV of the DG profit. However, the high capital cost of the new batteries as well as the dropping income reduction along the project lifetime may make the base case without the battery more profitable. In other words, the battery usage will be decreasing over the project lifetime as the potion of DG power requiring reschedule is dropping over the lifetime.

In this case, the idea of second life battery may be the adequate solution. Second life batteries have significantly cheaper capital costs compared to the new batteries, and their reduced life time, the main disadvantage of these batteries, is an advantage in this case. Thereby, the major driver for using SL batteries is the possibility of reducing costs and maximizing the DG investment by avoiding the utilization of new Li-ion batteries. The impacts of the second life battery utilization are compared to the new batteries; this is the core of the study presented in the next chapter.

Chapter 4

Enhancement of Photovoltaic DG Investment using Second Life Batteries

4.1 Introduction

The main goal of the research work presented in this chapter is to introduce the idea of integrating the second life batteries, which have lost part of their original performance during their first life, with the distribution system. The specific objective is to utilize the SL batteries for rescheduling the PV DG power in order to increase the DG penetration (minimize the active power curtailment) while fulfilling the utility technical constraints. Another objective is to use the SL batteries connected at the same bus of the DG to maximize the DG project investment.

Based on the work presented in Chapter (3), it was concluded that it is better for the DG investor to connect a large size DG and allow the utility to perform active power curtailment. This option achieves a higher profit compared to connect a small size DG less than the maximum allowable power injection specified by the utility. However, the results also showed high-profit reduction (10.82% - 12.3% of the profit NPV) due to this curtailment. This significant reduction introduces the idea of integrating battery energy storage to reschedule the PV DG power for the sake of maximizing the profit.

In this chapter, the idea of the integration of SL batteries with the distribution system to enhance the PV DG penetration and profit is proposed. The maximization problem for the incremental profit NPV (the difference between the profit NPV before and after the addition of the battery) is formulated. The optimization problem is solved, and the optimal battery size and operation schedule is obtained for different test cases; i.e. the fixed and variable energy prices. For all analysis presented, the SL batteries integration is compared to the brand-new batteries.

4.2 Modeling of the SL Batteries

The main difference, in terms of modeling, between the brand-new batteries and SL batteries is the deteriorated performance of the SL batteries. SL batteries have already consumed a part of their capacities during their first life which is known as capacity fading. Accurate modeling of the capacity degradation of the SL batteries plays a role in the determination of the lifetime duration of the battery in its second life, and hence it would provide more precise data for the second life planning.

4.2.1 Modeling of the Capacity Degradation of Batteries

Capacity degradation of EV batteries is dependent on several factors, such as the battery aging, operating temperature, battery chemical component, and size. However, the most effective factors that cause capacity fading are storage loss and the discharge cycle loss. The storage capacity loss is defined as the loss which happens to the battery with aging; even if the battery is not in operation. The discharge cycle loss is the capacity loss due to the discharging of the battery. Every discharge cycle of the battery contributes by a percentage in the capacity degradation for a certain depth of discharge (DoD). The depth of discharge is variable for every cycle based on the system requirements. For the new batteries, the DOD is recommended not to exceed 70% of the battery capacity; i.e. the state of charge is recommended not to be less than 30% of the capacity.

In order to calculate the capacity degradation of each cycle, equation (4.1) is used [75]. The equation describes the capacity degradation taking into consideration different factors affecting the capacity fading. The degradation of each cycle is dependent on the depth of discharge, the rate of discharge, the annual capacity fade that happens due to the storage, and the operating temperature at which the battery is used.

$$Capacity\ Dergadation = \left(\sum_{cy=1}^{CY} \left(f(DoD) * f(temp) * CapF\right)_{cy} + Cap_{storage} * Yr\right) * f(temp) \qquad (4.1)$$

Where:

$f(DoD)$: A factor that is corresponding to DOD.

$f(temp)$: Temperature factor.

$CapF$: A factor that is corresponding to capacity fading per cycle.

$Cap_{storage}$: the capacity fading due to storage per year

Yr : The number of service years of the battery.

cy: The number of discharge cycles.

CY: The total number of discharge cycles.

The aforementioned factors are discussed as follows;

A. Temperature Factor

Arrhenius model is used to model the capacity fading due to the temperature variation. The temperature factor could be calculated using (4.2). However, based on the surveyed studies, any operating temperature range between -20C and 40C has a minimal impact on the capacity fading rate. Therefore, in the proposed study, the temperature effect is considered negligible; i.e. the temperature factor is set to one.

$$f(temp) = \exp(-E_a / R(1/T - 1/T_{reference})) \tag{4.2}$$

Where:

E_a : The activation energy.

R : The gas constant.

T: the operating temperature during the cycle.

$T_{reference}$: The reference operating temperature.

B. Depth of Discharge Factor

The percentage of capacity fading affects the percentage of capacity degradation; e.g. the capacity fade corresponding to DoD=35% is less than the capacity fade corresponding to DoD=60%. In order to model the impact of the DOD on the capacity degradation, equations (4.3) and (4.4) are used [76]. The two equations present an approximate model for the percentage capacity fading for different ranges of DoD. Equation (4.3) is used when the DOD is greater than 51% of the battery manufacturing capacity, while (4.4) is used when the DOD is less than 51% of the battery manufacturing capacity.

$$f(DOD) = 1 + 0.025(\mathrm{DOD} - 51\%)\ ,\ \mathrm{DOD} \geq 51\% \tag{4.3}$$

$$f(DOD) = 1 - 0.025(51\% - \mathrm{DOD})\ ,\ \mathrm{DOD} < 51\% \tag{4.4}$$

C. Capacity Fading Factor

The capacity fading can be calculated through the fitting empirical formula of the second life Li-ion battery which represent the percentage capacity remaining after a number of cycles (*Cy)* regardless of the depth of the discharge. Equations (4.5) and (4.6) [75] could be used for calculating the capacity fading factor per cycle.

$$Capacity_{cy} = -4*10^{-10}*(cy)^3 + 3*10^{-6}*(cy)^2 - 0.008(cy) + 100.37 \quad (4.5)$$

$$CapF = Capacity_{cy} - Capacity_{cy-1} \quad (4.6)$$

D. Capacity Fading Due to storage

This factor represents the capacity degradation due to the aging of the battery regardless it was in service or not. Based on the practical testing results presented in [76], the factor corresponding to capacity fading capacity due to storage ($Cap_{storage}$) can be considered constant and equal to 0.033 of the manufacturing capacity per year. Thus, the capacity of the battery will be reduced by 0.033 of the original capacity for each year due to the aging factor only.

4.2.2 SL Battery Model

Based on the factors and equations presented in subsection 4.2.1, the SL battery model is introduced as follows;

A. SL Battery Starting Capacity

At the beginning of its second life, the capacity of the SL battery is assumed to be 80 % of the manufacturing capacity; i.e. 20 % capacity degradation. As shown in Figure 4.1 that is obtained from equation (4.5), a remaining capacity of 80.362 % is equivalent to a number of cycles of 5,500. Taking the aging effect into consideration, the SL batteries are usually sold after spending ten years on average during their first life. Thus, additional capacity fading of 0.33% (10 times 0.033) is deducted from the remaining capacity. To sum up, the initial capacity of SL batteries used in the presented study is 80 % of the rated capacity and this is considered equivalent to 5,500 cycles of discharge. Therefore, for the cycle counter, the initial value of cycles number will be set to 5,500 cycles; i.e. equation (4.5) will be changed to (4.7).

$$Capacity\ Dergadation = (\textstyle\sum_{cy=5001}^{CY} (f(DoD) * CapF)_n + (Cap_{storage} * Yr) \quad (4.7)$$

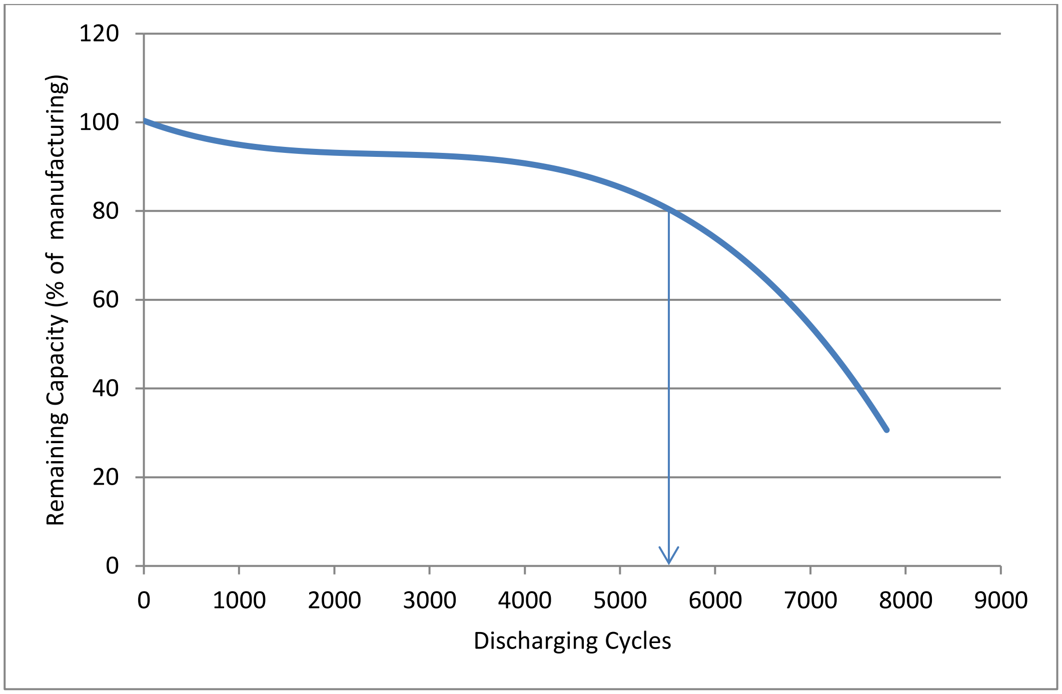

Figure 4.1 Battery fading

B. SL Battery Available Capacity

The available capacity for the SL battery is the difference between the starting capacity of the SL battery and the capacity threshold (i.e. minimum SOC). The majority of the batteries' manufacturers recommend that the SOC of the EV batteries should not be reduced beyond 30 % of the manufacturing capacity. This recommendation is to decrease the capacity degradation and to extend the battery lifetime. However, in the presented study, the available capacity of the SL battery is assumed to be equal to the total remaining capacity; i.e. 80% of the manufacturing capacity.

C. SL Battery Lifetime

The capacity beyond which the battery is not reliable and is not efficient for any application is set to be 30% of the manufacturing capacity. Thus, if the capacity degradation of the SL batteries reached 50% (in addition to the 20% degraded in the first life), the battery will be no longer usable and should be replaced. Therefore, in the presented work, the SL battery lifetime is determined in terms of used cycles, not in terms of years. As shown in Figure 4.1, the number of discharge cycles at which the battery is useless is approximate equals to 7,800 cycles (while neglecting the storage and DOD effects). Thus, during its second life, the battery could be used for 2,300 cycles only due to the dramatic degradation of the battery during its second life. The lifetime of the SL batteries will be dependent upon the application. Therefore, if the battery is used on a daily basis (i.e. 365 discharge cycles per year), the average lifetime will be 7.6 years. However, if the DOD is exceeding 51%, the SL battery will be degraded faster.

D. SL Battery Manufacturing Capacity and Price

There is a huge range of EV batteries' capacities from different EV manufacturers and makes. Moreover, the batteries capital costs vary based on the technology used and the EV make. In addition, the capacity in kWh and the power ratings in kW largely affects the battery price. Several studies [77] [tackled the pricing exercise of the SL batteries; the most common price of the SL battery fluctuates between 33% to 50% of the brand-new battery. For simplicity, the SL batteries used in the presented study are multiple of 30 kWh (manufacturing capacity), and the SL price is assumed to be 33 % of the brand-new battery (the price of the brand-new battery is in range of 130-228 C$/kWh for the year 2018). To conclude, the size of SL batteries used in the proposed work are multiples of 30 kWh (24 kWh starting capacity), and the per unit price is 33% of the brand-new battery (the SL battery price is 1,722 C$ based on 2018 prices and the new battery will cost 5,370 C$).

E. SL Battery Price Forecast

Since the batteries used in the proposed study is SL batteries, most likely they will be replaced during the project lifetime (i.e. 20 years). Therefore, it is very important to develop a forecast for the price variations of the SL batteries all over the twenty years. In other words, if the investor decided to purchase another SL battery in any year of the project, the price at this year should be estimated. It is well known that the batteries technology is mounting rapidly, and the batteries prices are falling dramatically. Thus, historical data for the average Li-ion battery price presented in Figure 4.2 is used to develop the price forecast. This data was collected from the Li-ion battery price survey conducted in [78]. The Trend of the historical data is obtained, and it found to be decaying exponential as shown in Figure 4.3. The forecast for the expected battery prices during the project lifetime is developed and the results are presented in Table 4-1

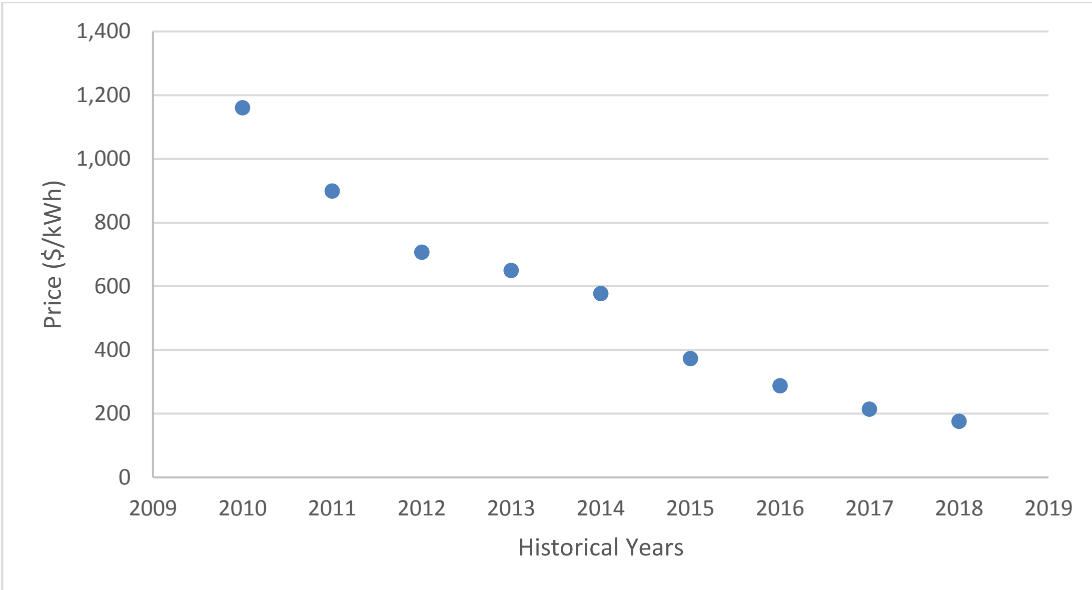

Figure 4.2 Historical Battery Prices

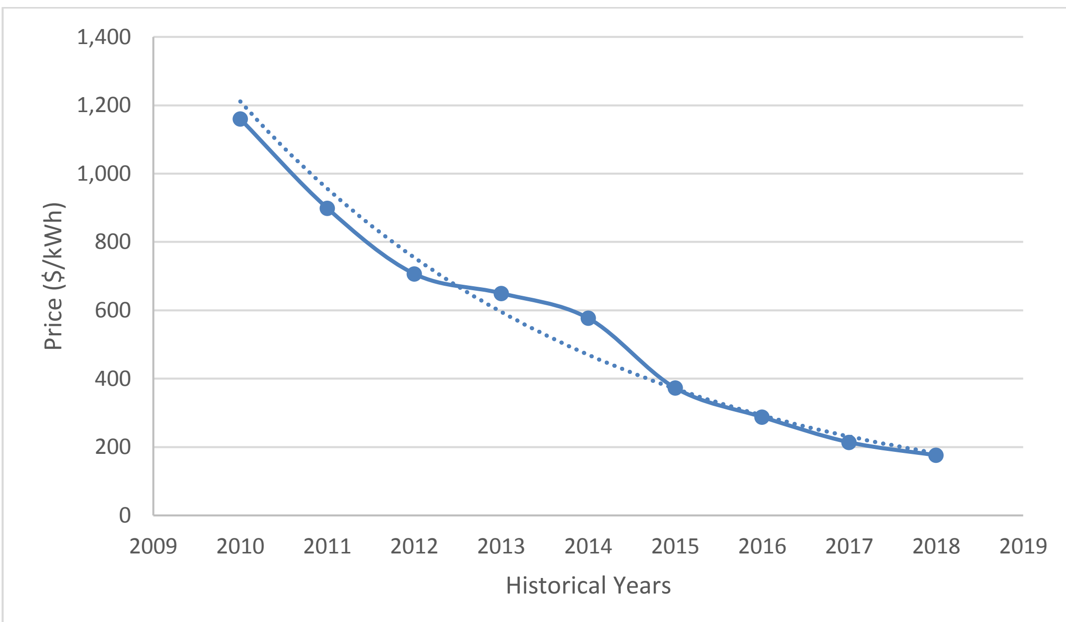

Figure 4.3 Exponential Trend of the Battery Price Variations

Table 4-1 New Battery Price Forecast

Year	Price ($/kWh)	Year	Price ($/kWh)
2019	144.32	2029	37.76
2020	119.79	2030	35.12
2021	100.62	2031	33.01
2022	85.53	2032	31.36
2023	73.55	2033	30.11
2024	63.99	2034	29.20
2025	56.31	2035	28.62
2026	50.12	2036	28.42
2027	45.11	2037	28.38
2028	41.05	2038	28.33

4.3 Battery Integration for Minimizing Active Power Curtailment

In this subsection, the battery is connected at the same bus of the PV DG to prevent the active power curtailment while minimizing the SL batteries cost. As determined from chapter (3), the optimal DG size to maximize the profit is 1000 kW. The expected PV DG power for this DG size as compared to the maximum allowable power curtailments is presented in Figure 4.4. It is clear that the maximum curtailment occurs at Spring season for the first year as shown in the typical day model for the Spring season presented in Figure 4.5. As shown in the figure, the maximum curtailed power is 299.1 kW and occurs at hour =13 (1:00 pm) and the maximum curtailed energy for one day is 1,474 kWh. Based on the curtailed energy, the optimal battery size is to be selected in order to minimize the net present value of the capital cost of the battery while maximizing the DG energy injected to the system. The optimal battery ratings should ensure that no power curtailment will occur for all seasons over the project lifetime. The optimization problem should consider the dramatic degradation of the SL battery; thus, the number of battery replacements over the project lifetime should be determined. The problem is formulated and solved in the following subsections.

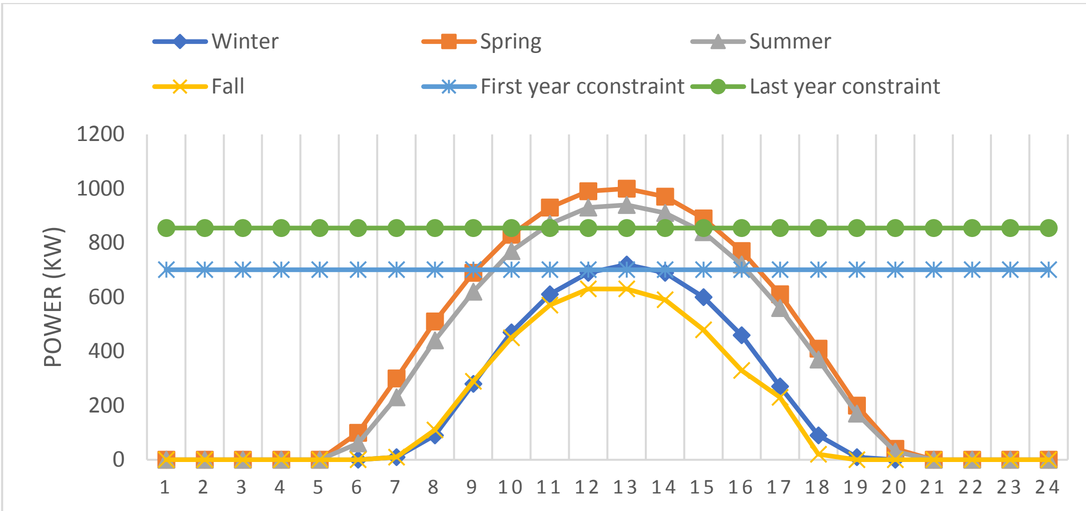

Figure 4.4 DG Power Profile for the Four Seasons

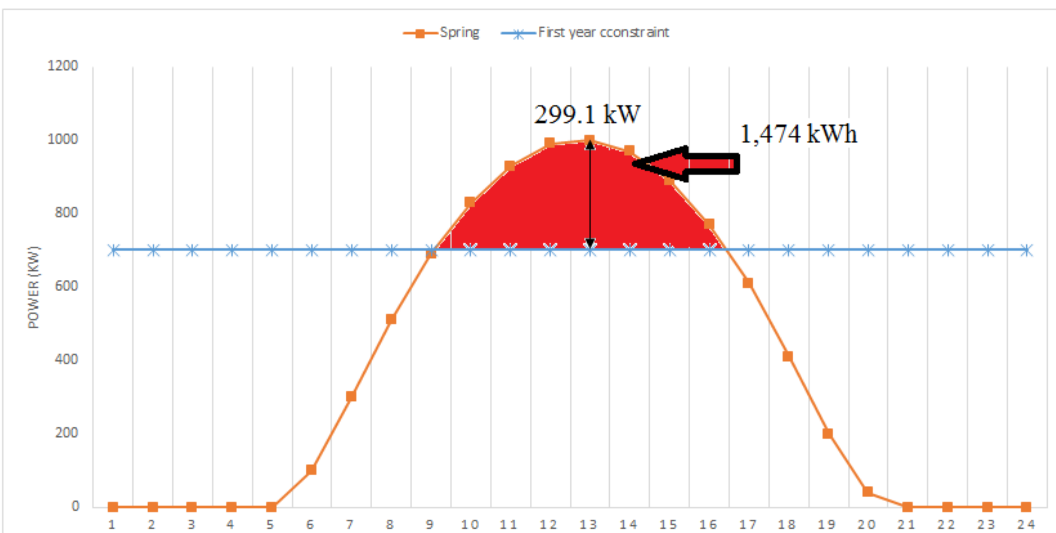

Figure 4.5 Curtailed Energy for Spring Season

4.3.1 Battery Cost Minimization Problem Formulation

The problem under study aims to determine the minimum net present value of the batteries capable of saving all the curtailed energies from the PV DG (for all seasons and all years). The objective of this problem is expressed in (4.8).

$$Min \sum_{b=1}^{RP} \frac{Cap\ Cost(y_b)}{(1+i)^{y_b}} \tag{4.8}$$

Where;

$Cap\ Cost$: is the capital cost of the battery.

y_b: is the year at which the battery is purchased and connected.

RP: is the total number of battery placements/ replacements required over the project lifetime.

i: is the interest rate

The following constraints are used;

$$E_{ch} = \eta_{ch} E_{c,max} \tag{4.9}$$

$$E_{cap} \geq E_{ch}\ \forall\ all\ seasons\ \forall\ all\ years \tag{4.10}$$

Where;

E_{ch}: is the energy to be stored in the battery during one day .

η_{ch}: is the charging efficiency.

$E_{c,max}$: is the maximum curtailed energy for one day.

E_{cap} : is the available capacity of the SL battery.

The constraints ensure that the battery available size is enough to store all the curtailed energy. It should be noted that the available battery size is decreasing due to capacity fading. Thus, the capacity of degradation per year is calculated using the degradation model presented in section 4.2.2. Here, the investor has two options; the first is to use a battery size just equals to the curtailed energy. This battery will suffer from high degradation due to the high DOD during every cycle. Therefore, the investor may require making one or two replacements for the SL batteries over the project lifetime. The second option is to use a larger battery size; thus, the DOD will decrease and consequently, the capacity degradation will do. Therefore, a smaller number of battery replacements are required. The solution of the optimization problem will advise the investor with the optimal battery size that minimizes the NPV of the batteries cost while saving all available energy from curtailment.

4.3.2 The Optimization Method

The Firefly optimization method is used for solving all optimization problems proposed in this chapter. The firefly optimization algorithm is inspired by the natural behavior of the fireflies; a firefly of the maximum brightness has the largest ability to attract other fireflies. The brightness of a firefly is affected or determined by the landscape of the objective function. For a maximization problem, the brightness can simply be proportional to the value of the objective function [79], whilst for a minimization problem; the brightness is inversely proportional to the value of the objective function. The brightest firefly is the best solution for the objective function, it attracts the other fireflies (other candidate solutions). In their journey, other fireflies may find a better solution for the objective function; therefore, the position of the brightest firefly changes. This process continues until all fireflies reach one optimal position (may be local or absolute optima) or until the allowable maximum number of iterations is reached.

The distance between the brightest firefly and the other fireflies, (r_{ij}) is calculated using (4.4)

$x_{i,k}, x_{j,k}$ are the positions of firefly *i* and *j*.

$$r_{ij} = \sqrt{\sum_{k=1}^{d} (x_{i,k} - x_{j,k})^2} \tag{4.11}$$

The brightest firefly (best solution within a certain iteration) attracts the less attractive one and the positions of the other fireflies are updated using (4.12)

$$x_i = x_i + \beta_0 \exp(-\gamma r_{ij}{}^2) \times (x_j - x_i) + \alpha(rand - \frac{1}{2}) \tag{4.12}$$

Where the first term is the old firefly position, the second term is used to update the firefly position based on the brightness of the fireflies and the third term is used to randomize the movement of Firefly. β0 is the initial attractiveness, γ is the absorption coefficient, the values of these parameters are determined according to the optimization problem. α is a randomization parameter that decreases at each iteration by equation (4.13) and rand is a random number generator uniformly distributed between [0,1].

$$\alpha^{k+1} = \alpha^{k} \left(\frac{1}{2K_{\max}}\right)^{1/k_{\max}} \tag{4.13}$$

4.3.3 The Proposed Technique for Capital Cost Minimization

The proposed optimization technique aims at determining the optimal battery that will minimize the net present value of battery costs (initial capital cost and extension costs) within the whole period of the project duration and prevent the curtailment of the DG power. The outputs of this technique are the optimal battery sizes and the corresponding installation year. The proposed technique is described in the following steps:

Step (1): Determine the energy curtailment for all seasons for all years over the project lifetime.

Step (2): Generate a set of random battery sizes (fireflies, i.e. each firefly has one dimension represents the battery size.). This set contains the candidate sizes of the batteries to be installed at the beginning of the project (year=0). The generated battery sizes should satisfy the constraint presented in (4.3); i.e. the battery capacity should be enough to store the maximum curtailed energy (energy curtailed from the spring season of the first year; Figure 4.5).

Step (3): For a generated battery size, calculate the degradation of the battery for each year using the DOD and equations (4.3) to (4.6).

Step (4): At a certain year y_b if the remaining battery size is less than the maximum curtailed energy at this year, a battery replacement is required. Therefore, set the replacement battery capacity to the nearest size just above the maximum curtailed energy at this year (year, y_b).

Step (5): Calculate the degradation of the replacement battery starting from year y_{b+1} up to the end of the project. If another battery replacement is required repeat step (4).

Step (6): Calculate the NPV of the installed batteries using (4.8).

Step (7): Repeat steps (3) to (6) for all remaining battery sizes of the generated set of random sizes.

Step (8): Determine the size that achieves the lowest NPV (the brightest firefly) and updates the other sizes using the updating equations (4.11) to (4.13).

Step (9): Repeat steps (3-8) until all sizes in the set converge to one optimal size.

Step (10): Set the battery size to be installed at the start of the project to the value obtained in (9) and calculate the battery degradation and the year of replacement.

Step (11): At the year of replacement, generate a new set of random battery sizes; this set contains the candidate sizes of the batteries to be installed at the year, y_b.

Step (12): Repeat Steps (3-11) to determine the optimal battery size at the replacement year; in the NPV calculations, the cost of the battery installed at the beginning of the project is fixed and determined based on the optimal size obtained from step (9).

Step (13): Repeat Steps (11) and (12) for any required replacements.

4.3.4 Results of the Optimal sizing of SL Batteries

As discussed earlier, the objective is to determine the optimal sizes of the batteries that will minimize the net present value of battery costs (Placement capital cost and successive replacements) within the whole period of the project duration and prevent the curtailment of the DG power. The optimization technique will determine the best solution among the following choices; the first is to choose a large size of the battery with a decent DoD. This large size of battery will prevent the battery from steep degradation, and therefore, remains for a will last for a larger number of years. The second choice is to choose a smaller size of the batteries that last for shorter periods, with deep DoD. Therefore, multiple replacements of these batteries are required over the project duration. The proposed technique is implemented in the field of MATLAB to find an answer to the aforementioned questions.

Table 4-2 Curtailed Energy Per Day for All Seasons

Year	Curtailed Energy (kWh)			
	Spring	Summer	Fall	Winter
2019	1,473.7	1,073.7	19.1	0
2020	1,404.4	1,004.4	9.2	0
2021	1,330.2	931.6	0	0
2022	1,275.6	884.8	0	0
2023	1,266.5	877	0	0
2024	1,212.6	830.8	0	0
2025	1,155.2	781.6	0	0
2026	1,118.8	750.4	0	0
2027	998.4	647.2	0	0
2028	965.4	619.5	0	0
2029	898.2	563.5	0	0
2030	867.0	537.5	0	0
2031	784.2	468.5	0	0
2032	736.8	429	0	0
2033	725.4	419.5	0	0
2034	693.0	392.5	0	0
2035	637.8	346.5	0	0
2036	578.5	288.8	0	0
2037	549.5	265.6	0	0
2038	506.5	231.2	0	0

First, the energy curtailment for all seasons for all years over the project lifetime are obtained and presented in Table 4-2. As shown from the table the curtailed energy is decreasing over the years due to the increasing constraint of the maximum allowable injected power. The available battery size at each year should be greater than maximum curtailed energy occurs in this year. However, taking the charging efficiency into consideration as declared in equation (4.9), the charging energy will be decreased by the charging efficiency. The charging efficiency is assumed to be 90%, and the minimum battery capacity that should be available at each year is obtained and presented in Table 4-3. It was assumed that a multiple of 24 kWh SL batteries (30 kWh manufacturing capacity) are only available; the minimum number of SL batteries at each year is determined and presented in Table 4-3.

Table 4-3   Minimum Battery Sizes

Year	Maximum Curtailed Energy (kWh)	Corresponding Charging Energy (kWh)	Minimum Battery Size (kWh)	Number of Battery Units
2019	1,473.7	1326.33	1344	56
2020	1,404.4	1263.96	1272	53
2021	1,330.2	1197.18	1200	50
2022	1,275.6	1148.04	1152	48
2023	1,266.5	1139.85	1152	48
2024	1,212.6	1091.34	1104	46
2025	1,155.2	1039.68	1056	44
2026	1,118.8	1006.92	1008	42
2027	998.4	898.56	912	38
2028	965.4	868.86	888	37
2029	898.2	808.38	816	34
2030	867.0	780.3	792	33
2031	784.2	705.78	720	30
2032	736.8	663.12	672	28
2033	725.4	652.86	672	28
2034	693.0	623.7	624	26
2035	637.8	574.02	576	24
2036	578.5	520.65	528	22
2037	549.5	494.55	504	21
2038	506.5	455.85	456	19

The optimization technique described in the previous subsection implemented and the optimal battery size and years of replacement were determined. Table 4-4 shows the obtained optimal values. The annual degradation of the SL batteries for this optimal scenario is obtained and presented in Table 4-5 and 4-6. The results show at the end of the 9th year, the SL battery connected at the beginning of the project is still in working conditions (i.e. the available capacity was greater than 30% of the manufacturing capacity). However, the available capacity in year #10 is less than the maximum charging energy in this year. Thus, to fulfill the constraint described in (4.9) and (4.10), battery replacement is required at the beginning of year #10.

Table 4-4 Optimal Battery Installation Scenario

Optimal Battery Size (kWh); manufacturing capacity	1,710	1,110
Connected at the beginning of Year #	1	10
Per unit price of the brand-new (C$/kWh)	144.32	41.05
Total price of the SL battery (C$)	81,439.78	15,036.62
Net Present Value of the total capital cost (C$)	92,964.08	

Table 4-5 Degradation of the First battery

Year	Maximum Charging Energy (kWh)	Annual Degradation (% of manufacturing capacity)	Cumulative Degradation (% of manufacturing capacity)	New Size of the battery at end of the year (kWh)
1	1326.33	2.21	2.21	1330.04
2	1263.96	2.47	4.69	1287.776
3	1197.18	2.73	7.4286	1240.97
4	1148.04	3.01	10.446	1189.367
5	1139.85	3.31	13.76	1132.695
6	1091.34	3.62	17.38	1070.74
7	1039.68	3.94	21.329	1003.268
8	1006.92	4.28	25.61	930.0168
9	898.56	4.63	30.24	850.8268
10	868.86	N/A	N/A	N/A

Table 4-6 Degradation of the second battery

Year	Maximum Charging Energy (kWh)	Annual Degradation (% of manufacturing capacity)	Cumulative Degradation (% of manufacturing capacity)	New Size of the battery at end of the year (kWh)
10	868.86	2.22	2.22	863.377
11	808.38	2.47	4.68	835.971
12	780.3	2.7	7.42	805.608
13	705.78	3.0	10.43	772.162
14	663.12	3.31	13.74	735.4585
15	652.86	3.6	17.36	695.3166
16	623.7	3.94	21.297	651.594
17	574.02	4.27	25.57	604.155
18	520.65	4.6	30.19	552.856
19	494.55	4.98617241	35.17933347	497.5093985
20	455.85	5.363425026	40.54275849	437.9753807

To clarify the importance of integrating the SL battery for minimizing the active power curtailment, the same task was performed using a brand-new battery. In this case, there is no need for battery replacement; i.e. one battery installed at the beginning of the project is enough. Moreover, there is no need for the optimization technique as the battery size is determined based on the maximum curtailed energy only. A comparison between the net present values of the SL battery scenario and the brand-new battery scenario is presented in Table 4-7. The comparison shows that the SL battery scenario achieves a 52.28 % savings in the costs while achieving the same task.

Table 4-7 Comparisons between SL and Brand-new Batteries

	Brand-new Battery Scenario	SL Battery Scenario
Optimal Battery Size (kWh); manufacturing capacity	1,350	1,710 at beginning of year #0 1,110 at beginning of year #10
Net Present Value of the total capital cost (C$)	194,832	92,964

In order to evaluate the impact of the integrated SL batteries on the investor income, the saving in curtailed energy is converted to C$. The fixed price scenario of 0.288 $/kWh is used to calculate the additional income achieved due to battery integration. The discharging efficiency of the battery is included in the calculations; a discharging efficiency of 90% is multiplied times the charging energy to calculate the energy discharged from the battery to the grid. Table 4.8 shows the present values of the additional income achieved due to battery installation. The net present value is 543,700 C$ which is 585% of the SL battery capital cost. These results clarify the significance of integrating the SL batteries with the system in terms of investment profits. This conclusion leads to the profit maximization analysis presented in the next section.

Table 4-8 Additional Income Due to SL Batteries

Year	Additional annual energy delivered to the grid (kWh)	The present value of the additional income (C$)	Year	Additional annual energy delivered to the grid (kWh)	The present value of the additional income (C$)
1	189,177	54,483	11	107,742	23,089
2	178,231	49,835	12	103,526	21,539
3	166,717	45,258	13	92,337	18,652
4	159,243	41,970	14	85,931	16,852
5	157,997	40,429	15	84,391	16,068
6	150,619	37,418	16	80,012	14,791
7	142,762	34,433	17	72,553	13,021
8	137,779	32,264	18	63,929	11,139
9	121,297	27,577	19	60,081	10,164
10	116,823	25,786	20	54,376	8,931

4.4 Incremental Profit Maximization

In this section, the effect of the SL batteries integration with the PV DG on the investment profit is evaluated. The objective is to determine the optimal battery size, charging/discharging schedule, and time of placement/replacement in order to maximize the investor profit. Since the investor is already achieving a profit from the selling the energy of the PV DG alone as discussed in chapter (3), the focus here will be on the incremental profit due to battery installation.

It was clarified in section (4.3) that the SL batteries increase the income, such that the additional income due to battery installation is 585% of the battery cost. Thus, it can be concluded that the battery size has a minor impact on the incremental profit as compared to the optimal battery schedule. In other words, the most important for the investor is to determine the optimal battery charging/discharging schedule that maximizes the income and consequently the profit as the battery cost is not affecting the profit that much. Therefore, the problem under study is formulated to maximize the income through determining the battery scheduling, and the battery size will be calculated based on the optimized schedule as shown in the following subsections.

4.4.1 Income Maximization Problem Formulation

The problem under study aims to determine the optimal battery charging/discharging schedule to maximize the investor income. The objective of this problem is expressed in (4.14) by considering the power of the DG and the battery fixed over one hour.

$$Max \sum_{h=1}^{24} [P_{DG}(hr) + P_{batterry}(hr)] \times \Pr(hr) \tag{4.14}$$

Where;

$P_{DG}(hr)$: is the DG output power

$P_{batterry}(hr)$: is the battery output power (+ve for discharging and -ve for charging)

$\Pr(hr)$: is the variable energy price described in chapter (3)

The problem is constrained by;

- The maximum allowable injected power (*MAIP*) constraint

$$P_{DG}(hr) + P_{batterry}(hr) \le MAIP \tag{4.15}$$

- The minimum injected power is zero; this means the battery cannot absorb energy from the grid and it can only be used for managing the PV DG energy.
- The battery SOC constraint; the SOC at the start and the end of the day must be equal (assumed to be 50% of the available capacity); i.e. the sum of charging and discharging battery powers should be zero.

$$\sum_{hr=1}^{24} P_{batterry}(hr) = 0 \tag{4.16}$$

The optimization problem is solved using the firefly optimization method where the fireflies here are the candidate battery powers at each hour. The problem is solved for each typical day separately; i.e. the problem is solved 80 times (4 season typical days per year X 20 years). Based on the optimal battery schedule, the corresponding capacity required to accommodate this schedule is calculated for each solution of the 80 solutions. Then, based on the capacity degradation model, the best sizes of the SL batteries are obtained along with the replacement times. In other words, two replacements are only allowed over the project lifetime (as the expected lifetime of the SL battery is 7.6 years in case of 365 cycles per year as discussed in section 4.2.2). If the battery size is adequate for the battery schedule, but its capacity degradation is high and cause more than two replacements, the upper battery size will be used.

4.4.2 Results of the Profit Maximization

The optimization problem is solved in MATLAB and the optimal charging/discharging schedules for all seasons and years are obtained based on the variable energy prices discussed in chapter (3). To simplify the problem the charging/discharging efficiencies were assumed to be 100% and the battery rated powers were left unconstrained. The optimal battery schedules for the four seasons for the first year of the project are presented in Figures. 4.6 to 4.9. Moreover, the total injected power (i.e. the sum of the PV DG and the battery powers) for the spring season is compared to the PV power and presented in Figure 4.10. In all figures, the power flow to the battery is -ve (i.e. charging) and the power flow from the battery is +ve (i.e. discharging).

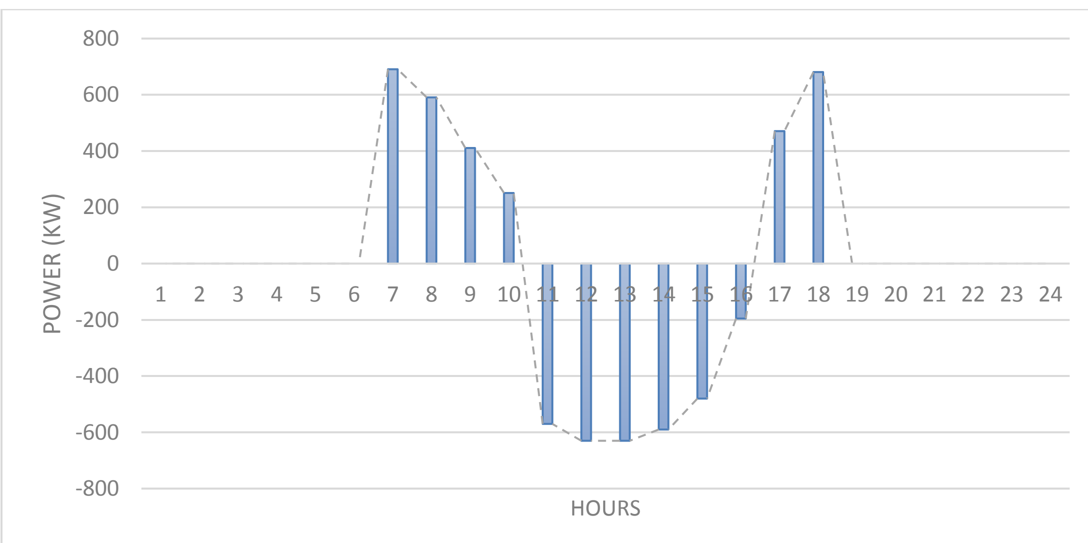

Figure 4.6 Battery schedule for Winter Season

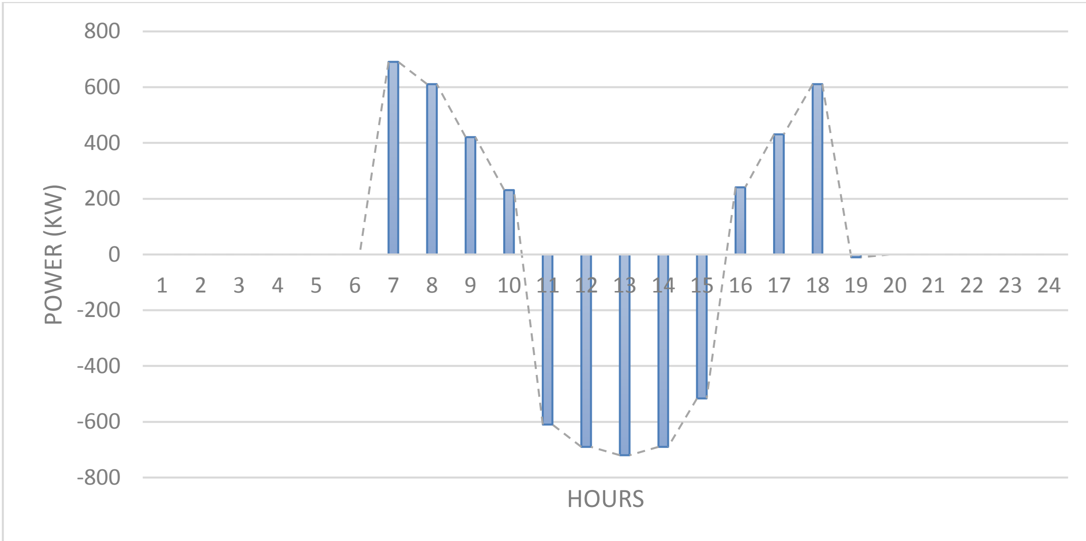

Figure 4.7 Battery schedule for Fall Season

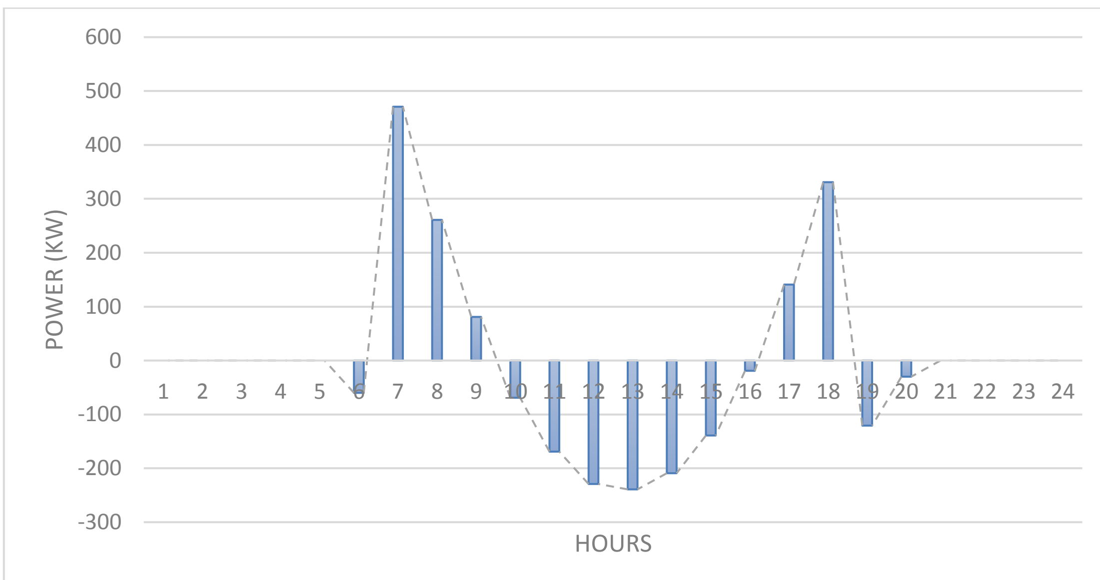

Figure 4.8 Battery schedule for Summer Season

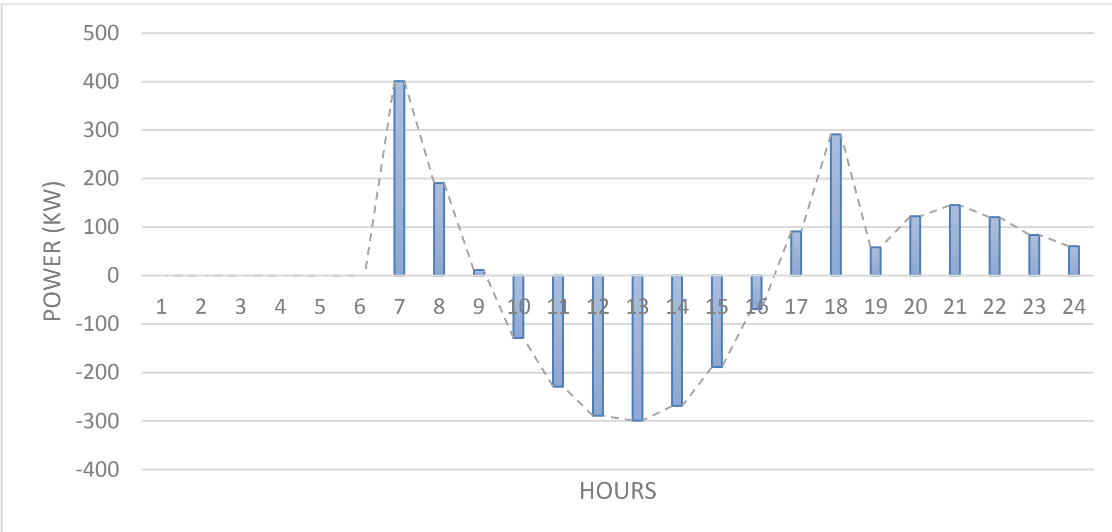

Figure 4.9 Battery schedule for Spring Season

Figure 4.10 Total Injected Power for Spring Season

It can be noted that the highest battery powers are in the winter and fall seasons; this is due to the energy prices. In the Winter and Fall, the peak PV DG power coincides with the mid-peak energy prices (hours 11 to15 and price of 0.2375 C$/kWh), therefore, the battery absorbs energy occurs at the mid-peak prices and discharge it at the peak energy prices (hours 7 to11, 15 to 16 and price of 0.33 C$/kWh). This is not the case for the Summer and Spring seasons, as the peak PV DG power coincides with the peak energy prices. However, for Summer and Spring, the PV DG generated power is higher than the MAIP constraint. Thus, the battery absorbs the amount of energy above the MAIP and redistributed it in the mid-peak price hours. This is obvious in Figure 4.9, as the total injected power to the grid is shaved to the MAIP (i.e. 700.9 kW). This shaved energy is rescheduled in the mid-peak hours; the amount of shaved energy is sufficient to settle the injected power to the MAIP for all mid-peak hours, and the remaining energy is injected during the off-peak hours.

The required battery capacity to achieve the optimal battery schedule is calculated based on the schedule and the assumption of the SOC (SOC at the first hour of the day is assumed to be 50% of the available capacity). Therefore, for the Fall season, for example, the 50% SOC covers the discharging occurs at hours 7-10; see Figure 4.7. The total discharging energy during these hours is 1,953 kWh. Since this energy is corresponding to 50% of the available capacity; then the available capacity should be at least 3,907 kWh. As previously defined, the available capacity of the SL battery is 80% of the manufacturing capacity, then the later should be at least 4,884 kWh. The manufacturing capacity of the SL battery, as a multiple of the 30-kWh unit, is then determined to be 4,890 kWh. The discusses sizing algorithm is executed to the 80 battery schedules obtained (4 Seasons X 20 years), and the highest size among the four seasons is determined for each year. Moreover, the obtained SL battery capacity is tested to determine the capacity degradation and the remaining capacity at each year. Based on this capacity degradation analysis, the best battery sizing scenario is obtained, and the purchasing costs are determined as presented in Table 4-9. We can note that the required battery capacity is increasing over the project lifetime, this occurs as the MAIP constraint is relaxed over the project lifetime. Thus, the battery can inject higher power and higher energy in return. However, thanks to the falling battery costs, the corresponding battery costs are significantly lower than the cost of the battery installed at the beginning of the project. Here appears the importance of the SL batteries, as they give the chance to the investor to purchase batteries at very low prices at later years of the project rather than purchasing all required batteries at the beginning of the project (the case of brand-new batteries).

Table 4-9 Required SL Battery Capacity and Costs

SL Battery capacity (kWh)	Installation Year	Cost (C$)
5,340	Beginning of 1st year	254,285
6,000	Beginning of 8th year	99,237
6,180	Beginning of 15th year	61,406

To evaluate the impact of the SL batteries on the incremental income and the incremental profit, the new income is calculated for each year based on the optimized power schedule (the sum of PV DG and battery). Then the incremental income is calculated as the difference between incomes before and after battery installation. The NPV of the incremental income, as well as the NPV of the SL battery cost, are calculated to determine the NPV of the incremental profit. The NPV calculations are presented in Table 4-10; the total NPV for the incremental profit is 1,059,891 C$ which proves the importance of the SL battery integration. In the case of the brand-new batteries, the required battery size is 4,950 kWh and the corresponding cost is 714,285 C$. All these costs should be paid at the beginning of the project; thus, the total NPV of the incremental profit is 721,177 C$. This show the superiority of using the SL batteries over the brand-new for this application as they achieve 47% more profit as compared to the new batteries.

Table 4-10 Net Present Value of the Incremental Profit

Year	Incremental Income (C$)	Battery costs (C$)	The present value of incremental income (C$)	The present value of battery costs (C$)	The present value of Profit (C$)
1	107,342	254,285	104,216	254,285	-150,070
2	106,176		100,081	0	100,081
3	104,568		95,694	0	95,694
4	103,088		91,592	0	91,592
5	102,825		88,698	0	88,698
6	101,268		84,810	0	84,810
7	99,609		80,991	0	80,991
8	98,558	99,238	77,802	80,689	-2,887
9	96,371		73,860	0	73,860
10	95,697		71,207	0	71,207
11	93,842		67,794	0	67,794
12	93,181		65,355	0	65,355
13	91,209		62,109	0	62,109
14	90,205		59,636	0	59,636
15	89,963	61,406	57,744	40,597	17,147
16	89,277		55,634	0	55,634
17	87,776		53,106	0	53,106
18	86,097		50,573	0	50,573
19	84,960		48,452	0	48,452
20	83,275		46,107	0	46,107
Net Present Value of the Incremental Profit (C$)					1,059,891

4.5 Summary

This chapter presented an innovative application of the SL batteries in the distribution grid. A comprehensive model for the SL batteries that considers the capacity degradation due to several factors were presented. Based on the capacity degradation model, the SL batteries were integrated to achieve two separate objectives; minimizing the curtailed energy and maximizing the investor profit. The two optimization problems were solved in MATLAB and the results show a significant advantage of the SL batteries over the brand-new ones. The main advantage of the SL batteries is that they give the chance to the investor to purchase batteries at very low prices at later years of the project rather than purchasing all the required batteries at the beginning of the project.

Chapter 5
Conclusion and Future Work

5.1 Summary of the Work

The proposed study aimed to integrate batteries, which have lost part of their original performance during their first life, with the distribution system applications. Two main objectives were formulated and solved; the first was to minimize the capital cost of the SL batteries required for smoothing the PV DG power in order to increase the DG penetration while fulfilling the utility technical constraints. The second objective was to use the SL batteries connected at the same bus of the DG to maximize the investment profit though maximizing the investment income.

The following research works were developed and presented throughout the proposed study;

A long-term load forecasting technique: used to forecast the distribution system loading conditions and to determine the maximum allowable injected power constraints for each year of the project lifetime.

- A probabilistic modeling strategy for PV power that considers their stochastic nature: this strategy was used to determine the expected PV powers for all hours and seasons. In other words, the typical day models for all season were obtained in order to calculate the PV DG income and amount of energy to be curtailed.
- A procedure to select the best DG size that achieves the maximum net present value of the DG profit while maintaining the distribution system technical constraints.
- A novel model for the SL batteries that consider their capacity degradation due to charging/discharging cycles, DOD, and storage factor. Moreover, the falling prices of the batteries were forecasted and included in the model.
- An optimization technique to determine the optimal SL batteries capacity in order to minimize the capital cost while smoothing the PV DG power and minimizing curtailed energy.
- An optimization technique to determine the operation schedule of the SL batteries required to maximize the DG investment profit.

5.2 Conclusions and Contributions

The presented research work proposed a novel idea which is the integration of SL batteries with the distribution grid. Although few studies used the SL battery for different application, none of them used the SL batteries for smoothing the PV DG power and maximizing the investor profit. The presented work used a comprehensive model of the SL batteries that consider their starting capacity, capacity fading, lifetime, and price forecast. The main conclusion derived from the presented study is that the SL batteries are adequate for the application and they have superiority over the brand-new batteries in terms of cost. Although the SL batteries suffer from very high capacity degradation compared to the new batteries, they give the chance to the investor to purchase batteries at very low prices at later years of the project rather than purchasing all the required batteries at the beginning of the project. Thus, it can be concluded that the SL batteries offer a competitive solution for the cost problems associated with the battery integration with the distribution systems. Therefore, this hot research topic should be studied from different perspectives to ensure the reliability of the SL batteries for utilization for different power system applications.

5.3 Future Work

The usage of the SL batteries that spent a part in their life in an automotive application, for different applications, has a great potential due to the proliferated numbers of the electric vehicles. Therefore, a huge number of SL batteries are expected to be disposed of in the next few years. The distribution system can acquire some benefits from adopting the usage of the SL batteries; however, this requires several studies. The proposed study tackled the idea of smoothing the PV power and improving profit. However, this idea should be comprehensively studied to ensure its suitability in terms of reliability and security. We suggest a study that evaluates the failure rate of the SL batteries to determine their impact on the distribution system reliability. Moreover, the usage of SL batteries on the residential scale to minimize the electricity bill would be very beneficial for the utility to decrease the peak demand and defer the substations upgrade.

Bibliography

[1] Maria C. Argyroua, Paul Christodoulidesb, Soteris A. Kalogirouc," Energy storage for electricity generation and related recesses": Technologies appraisal and grid scale applications", renewable and sustainable energy review 94 (2018), pp 804-821.

[2] Chen H, Cong TN, Yang W, Tan C, Li Y, Ding Y., "Progress in electrical energy storage system": a critical review. Prog Nat Sci (2009); pp. 291–312.

[3] Hadjipaschalis I, Poullikkas A, Efthimiou V., "Overview of current and future energy storage technologies for electric power applications". Renew Sustain Energy Rev (2009); pp.1513–1522.

[4] Poullikkas A. "Optimization analysis for pumped energy storage systems in small isolated power systems". J Power Technol (2013); 93, pp.78–89.

[5] Kousksou T, BruelP, JamilA, ElRhafiki T, ZeraouliY. "Energy storage: applications and challenges". Sol Energy Mater Sol Cells (2014);120, pp.59–80.

[6] Ekman CK, Jensen SH. "Prospects for large scale electricity storage in Denmark". Energy Convers Manag. (2010); 51, pp.1140–1147.

[7] Luo X, Wang J, Dooner M, Clarke J, Krupke C. "Overview of current development in compressed air energy storage technology". Energy Procedia (2014); 62, pp. 603–611.

[8] Beaudin M, Zareipour H, Schellenberglabe A, Rosehart W. "Energy storage for mitigating the variability of renewable electricity sources: an updated review". Energy Sustain Dev (2010); 14, pp.302–314.

[9] Ibrahim H, Ilinca A, Perron J., "Energy storage systems - characteristics and comparisons". Renew Sustain Energy Rev (2008), 12, pp.1221–1250.

[10] Mousavi GSM, Faraji F, Majazi A, Al-Haddad K. "A comprehensive review of flywheel energy storage system technology". Renew Sustain Energy Rev (2017), 67, pp. 477–490.

[11] Masaud TM, Lee KLK, Sen PK. "An overview of energy storage technologies in electric power systems: What is the future?" In: Proceedings of the North American Power Symposium (NAPS). IEEE, 2010, p. 1–6.

[12] Angheliţă P, Chefneux M, Balaban R, Trocan L. "Energy storage systems for buildings equipped with photovoltaic cells." In: Proceedings of the 3rd International Symposium on Electrical and Electronic Engineering (ISEEE), IEEE; 2010, p. 332–5.

[13] Carrasco JM, Franquelo LG, Bialasiewicz JT, Galván E, Guisado RCP, Prats ÁM, et al. “Power-electronic systems for the grid integration of renewable energy sources: a survey”. IEEE Trans Ind Elec. (2006); 53 , pp. 1002–1016.

[14] Yekini Suberu M, Wazir Mustafa M, Bashir N., “Energy storage systems for renewable energy power sector integration and mitigation of intermittency”. Renew Sustain Energy Rev (2014), 35, pp.499–514.

[15] Luo X, Wang J, Dooner M, Clarke J., “Overview of current development in electrical energy storage technologies and the application potential in power system operation”. Applied Energy (2015),137, pp. 511–36.

[16] Cho J, Jeong S, Kim Y. “Commercial and research battery technologies for electrical energy storage applications”. Prog. Energy Combust Sci (2015), 48, pp.84–101.

[17] International Electrotechnical Commission (IEC). Electrical Energy Storage: white paper. Switzerland; 2011.

[18] Dunn B, Kamath H, Tarascon J-M. “Electrical energy storage for the grid: a battery of choices”. Science (2011), 334, pp. 928–935.

[19] Poullikkas A. “A comparative overview of large-scale battery systems for electricity storage.” Renew Sustain Energy Rev (2013), 27, pp.778–788.

[20] Amirante R, Cassone E, Distaso E, Tamburrano P. “Overview on recent developments in energy storage: mechanical, electrochemical and hydrogen technologies”. Energy Convers Manag. (2017),132, pp.372–387.

[21] Daim TU, Li X, Kim J, Simms S. Evaluation of energy storage technologies for integration with renewable electricity: quantifying expert opinions. Environ Innov Soc Transit 2012;3:29–49.

[22] Naish C, McCubbin I, Edberg O, Harfoot M. Outlook of energy storage technologies. Eur Parliam Comm Ind Res Energy 2008.

[23] Seo H-R, Kim G-H, KimS-Y, KimN, Lee H-G, HwangC, et al. Powerquality control strategy for grid-connected renewable energy sources using PV array and supercapacitor. In: Proceedings of the international conference on electrical machines and systems. 2010: pp. 437–41.

[24] Ghiassi-Farrokhfal Y, Keshav S, Rosenberg C, Ciucu F. Solar power shaping: an analytical approach. IEEE Trans Sustain Energy 2015;6:162–70.

[25] Senjyu T, Datta M, Yona A, Funabashi TPV. Output power fluctuations smoothing and optimum capacity of energy storage system for PV power generator. Icrepq Com 2008:3–7.

[26] Toledo OM, Oliveira Filho D, Diniz ASAC. Distributed photovoltaic generation and energy storage systems: a review. Renew Sustain Energy Rev 2010;14:506–11.

[27] International Energy Agency (IEA). Technology Roadmap: Energy Storage.

[28] Zahedi A. Maximizing solar PV energy penetration using energy storage technology. Renew Sustain Energy Rev 2011;15:866–70.

[29] Argyrou MC, Christodoulides P, Marouchos CC, Kalogirou SA, Florides GA, Lazari L. Overview of energy storage technologies and a short-term storage application for wind turbines. In: Proceedings of the 26th international ocean and polar engineering conference and international society of offshore and polar engineers; 2016, p. 444–52.

[30] Rohit AK, Rangnekar S. An overview of energy storage and its importance in Indian renewable energy sector: part II – energy storage applications, benefits and market potential. J Energy Storage 2017;13:447–56.

[31] Aneke M, Wang M. Energy storage technologies and real life applications – a state of the art review. Appl Energy 2016;179:350–77.

[32] Castillo A, Gayme DF. Grid-scale energy storage applications in renewable energy integration: a survey. Energy Convers Manag 2014;87:885–94.

[33] Díaz-González F, Sumper A, Gomis-Bellmunt O, Villafáfila-Robles R. A review of energy storage technologies for wind power applications. Renew Sustain Energy Rev 2012;16:2154–71.

[34] Battery and Energy Technologies: Grid Scale Energy Storage Systems n.d.⟨http://www.mpoweruk.com/grid_storage.html.

[35] Lahyani A, Venet P, Guermazi A, Troudi A. Battery/Supercapacitors combination in uninterruptible power supply (UPS). IEEE Trans Power Electron 2013;28:1509–22

[36] Second life batteries lifespan: Rest of useful life and environmental analysis Lluc Canals Casalsa,b,∗, B. Amante Garcíaa, Camille Canalc

[37] Vilayanur V. Viswanathan and Michael Kintner-Meyer, "Second Use of Transportation Batteries: Maximizing the Value of Batteries for Transportation and Grid Services" IEEE TRANSACTIONS ON VEHICULAR TECHNOLOGY, VOL. 60, NO. 7, SEPTEMBER 2011

[38] Williams B, Lipman T. Analysis of the Combined Vehicle - Use Value of Lithium-Ion Plug-In-Vehicle Propulsion Batteries. Task 3, Second Life Applications and Value of 'Traction' Lithium Batteries., Tech. rep., California Energy Commission Prepared: Public Interest Energy Research (PIER) Program (2011).

[39] Neubauer, Pesaran. The ability of battery second-use strategies to impact plug-in electric vehicle prices and serve utility energy storage applications. Journal of Power Sources 196 (23).

[40] Neubauer J, Pesaran A, Williams B, Ferry M. A Techno-Economic Analysis of PEV Battery Second Use: Repurposed-Battery Selling Price and Commercial and Industrial End-UserValue. in:SAE 2012WorldCongress&Exhibition,2012.

[41] Neubauer, J., Smith, K., Wood, E., & Pesaran, A. Identifying and Overcoming Critical Barriers to Widespread Second Use of PEV Batteries. The United States.

[42] Eyer J, Corey G. Energy storage for the electricity grid: Benefits and market potential assessment guide.Tech.Rep.February,Sandia NationalLaboratories(2010).

[43] E. Martinez-Lasernaa,, I. Gandiagaa, E. Sarasketa-Zabalaa, J. Badedab,c,d, D.-I. Stroee, M. Swierczynskie, A. Goikoetxeaf "Battery second life: Hype, hope or reality? A critical review of the state of the ar"t, renewable & sustainable energy reviews. Vol 93, 2018,701-7018

[44] Debnath UK, Ahmad I, Habibi D. Quantifying economic benefits of second life batteries of gridable vehicles in the smart grid. Int J Electr Power Energy Syst 2014;63:577–87.

[45] Viswanathan VV, Kintner-Meyer M. Second use of transportation batteries: maximizing the value of batteries for transportation and grid services. IEEE Trans Veh Technol 2011;60(7):2963–70.

[46] Beer S, Gomez T, Dallinger D. An economic analysis of used electric vehicle batteries integrated into commercial building microgrids. IEEE Trans Smart Grid 2012;3(1):517–25.

[47] Lacey G, Putrus G, Salim A. The use of second life electric vehicle batteries for grid support EUROCON, 2013 IEEE July 2013 1255 1261

[48] Assunção A, Moura PS, de Almeida AT. Technical and economic assessment of the secondary use of repurposed electric vehicle batteries in the residential sector to support solar energy. Appl Energy 2016;181:120–31.

[49] Saez-De-Ibarra A, Martinez-Laserna E, Koch-Ciobotaru C, Rodriguez P, Stroe D-I, Swierczynski M. Second life battery energy storage system for residential demand response service. In: Proceedings of the IEEE international conference on industrial technology, vol. 2015-June 2015.

[50] Wolfs P. An economic assessment of second use lithium-ion batteries for grid support. In: Proceedings of the 20th Australasian Universities Power Engineering Conference (AUPEC); 2010. URL ⟨http://ieeexplore.ieee.org/xpls/abs_all.jsp? Arnumber=5710689⟩.

[51] Shokrzadeh S, Bibeau E. Repurposing batteries of plug-in electric vehicles to support renewable energy penetration in the electric grid. In: Proceedings of SAE 2012 World Congress and Exhibition

[52] Gladwin D, Gould C, Stone D, Foster M. Viability of second-life use of electric and hybridelectric vehicle battery packs IECON Proceedings (Industrial Electronics Conference); 2013. pp. 1922–7

[53] Tong SJ, Same A, Kootstra Ma, Park JW. Off-grid photovoltaic vehicle charge using second life lithium batteries: an experimental and numerical investigation. Appl Energy 2013;104:740–50.

[54] Kootstra MA, Tong S, Park JW. Photovoltaic grid stabilization system using second life lithium battery. Int J Energy Res 2015.

[55] Baumhöfer T, Brühl M, Rothgang S, Sauer DU. Production caused variation in capacity aging trend and correlation to initial cell performance. J Power Sources 2014;247:332–8.

[56] Schuster SF, Brand MJ, Berg P, Gleissenberger M, Jossen A. Lithium-ion cell-to-cell variation during battery electric vehicle operation. J Power Sources 2015;297:242–51.

[57] LihW,Yen J.Second-useApplications ofLithium-ionBatteriesRetiredfromElectric Vehicles: Challenges, Repurposing Process, Cost Analysis and Optimal Business. International Journal of Advancements in Computing Technology

[58] Omar N, Daowd M, Hegazy O, Geukens B, Timmermans JM, Coosemans T, Van den Bossche, P., VanMierlo J. Assessment ofsecond lifeof lithiumiron phosphate based batteries. International Review of Electrical Engineering 7 (April).

[59] Rohr S, Müller S, Baumann M, Kerler M, Ebert F, Kaden D, et al. Quantifying uncertainties in reusing lithium-ion batteries from electric vehicles. Procedia Manuf 2017;8(October (2016)):603–10.

[60] Swierczynski M, Stroe DI, Laserna EM, Sarasketa-Zabala E, Timmermans JM, Goutam S, et al. The Second life ageing of the NMC/C electric vehicle retired Li-ion batteries in the stationary applications. ECS Trans 2016;74(1):55–62.

[61] Martinez-Laserna E, Sarasketa-Zabala E, Stroe D, Swierczynski M, Warnecke A., Timmermans JM,Goutam S, Rodriguez P. Evaluation of Lithium-ion Battery Second Life Performance and Degradation. In: Proceedings of IEEE Energy Conversion Congress and Expo.

[62] Liao Q, Mu M, Zhao S, Zhang L, Jiang T, Ye J, Shen X, Zhou G. Performance assessment and classification of retired lithium ion battery from electric vehicles for energy storage. International Journal of Hydrogen Energy

[63] USABC, USABC Electric Vehicle Battery Test Procedures Manual, Revision 2. Tech. rep., USABC (1996).

[64] Saxena S, Le Floch C, MacDonald J, Moura S. Quantifying EV battery end-of-life through analysis of travel needs with vehicle powertrain models. J Power Sources 2015;282:265–76.

[65] International Energy Agency (IEA), Clean Energy Ministerial, Electric Vehicles Initiative, Global EV Outlook: Understanding the Electric Vehicle Landscape to 2020. Technical Report April; 2013

[66] Sathre R, Scown CD, Kavvada O, Hendrickson TP. Energy and climate effects of second-life use of electric vehicle batteries in California through 2050. J Power Sources (2015), pp.82–91.

[67] Ahmadi L, Fowler M, Young SB, Fraser Ra, Gaffney B, Walker SB. Energy efficiency of Li-ion battery packs re-used in stationary power applications. Sustain Energy Technol Assess (2014), pp.9–17.

[68] E. Martinez-Laserna et al., Technical Viability of Battery Second Life: A Study from the Ageing Perspective, in IEEE Trans. on Ind.App.

[69] M. T. Hagen and S. M. Behr, “The time series approach to time series load forecasting”, IEEE Trans.,(1987), pp. 785-791.

[70] G. Dudek, “Pattern-based local linear regression models for short-term load forecasting,” Electric Power Syst. Research, (2016), pp. 139-147.

[71] Dedinec, S. Filiposka, A. Dedinec, and L. Kocarev, “Deep belief network based electricity load forecasting: An analysis of Macedonian case,” Energy, (2016), pp. 1688-1700.

[72] Moghram and S. Rahman, “Analysis and evaluation of five short-term load forecasting techniques,” IEEE Trans. Power Syst., (1989), pp. 1484-1491.

[73] M. M. Othman, M. H. Ahmed and M. M. A. Salama, "A Probabilistic Economic Assessment Approach for Active Power Curtailment of Photovoltaic Based Distributed Generators," 2018 IEEE Power & Energy Society General Meeting (PESGM), Portland, OR, 2018, pp. 1-5.

[74] SLK60P6L SLV/WHT 220W-255W Poly-Crystalline Solar Modules. Siliken Canada. [Online]. Available: http://www.highlandsolar.ca/media/SLK60P6L with Linear Warranty.pdf

[75] Uttam Kumar Debnath , Iftekhar Ahmad, Daryoush Habibi, ” Quantifying economic benefits of second life batteries of gridable vehicles in the smart grid”. Electrical Power and Energy Systems 63 (2014) 577–587.

[76] Smith K, Markel T, Pesaran A. PHEV battery trade-off study and standby thermal control. In: 26th International battery seminar and exhibit, Fort Lauderdale, FL, USA, 16–19 March; 2009.

[77] Antonio Merino Rodriguez, “Optimization analysis of second-life batteries integration in fast-chargers for electric vehicles in Spain”, Master thesis.

[78] https://about.bnef.com/blog/behind-scenes-take-lithium-ion-battery-prices/

[79] X.-S. Yang, "Firefly algorithms for multimodal optimization," Stochastic Algorithms: Foundation and Applications SAGA 2009, vol. 5792, pp. 169-178, 2009.